Master thesis

Mechanics of multi-layer cellular system

Ariel Avanzi

Advisor: Amin Doostmohammadi

Submitted: August 15, 2023

This thesis has been submitted to The Faculty of Science, University of Copenhagen

To my beloved grandmother Ida

Abstract

Cellular systems in Nature are inherently three-dimensional and can be modeled as multi-layer of soft cells that are able to convert energy into mechanical forces that are used to move and modify their environment. This ability, known as activity, drives numerous dynamical processes, such as tissue morphogenesis, and wound healing. Aggregates of cells coordinate their behavior to collectively self-organize in a variety of different patterns, that are the foundation of life as we know.

This study introduces a 3D phase field model that is based on cellular deformation and the transmission of mechanical forces both within and beyond the layers of cells. The interactions are captured by adhesion and repulsion at the cell interface and an interacting solid scaffold is introduced to understand tissue formation on a substrate.

The numerical implementation shows the criteria that allow the cells to merge into a single layer, pointing out the relevance of cellular re-organization, while different patterns arise from the analysis of its mechanics. Forces and stresses that arise locally, are transmitted to the whole multicellular system, showing coordination in response to a change in the environment. The same type of collective response is driving the system in different configurations according to the degree of activity of the cells, highlighting the importance of this ability.

The main purpose of this thesis has been to construct a valid framework for understanding complex multilayer cellular phenomena. Starting from this general framework, more layers of complexity can be added to account for more complex geometries, and different cellular interactions within cells and beyond.

Keywords: multi-layer, cellular system, activity, mechanical forces, tissue morphogenesis, phase field, adhesion, active matter, substrate, collective behavior

Acknowledgements

Contents

Chapter 1

Introduction

Biological Importance

> *"The collective dynamics of cellular systems has gathered increasing attention over the last decades [1], inspiring experimental, theoretical, and numerical studies in an attempt to unravel the underlying physical principles. Single cells are able to convert chemical energy into mechanical forces [2], allowing them to move and modify their local microenvironment [3]. At the multicellular level, these forces are transmitted over tens of cell lengths [4], driving non-local cellular flows [5], which self-organizes into a vast range of patterns."*[6]

Collective dynamics arise from the ability of cells to self-organize and to drive numerous processes such as tissue morphogenesis [7], wound healing [8], and tumor progression[9, 10]. For instance see figures 1.2 and 1.1. This **collective behavior** can be seen as simultaneous changes in multiple individuals, id est collective, in the same environment, that are hard to restore on the bare individual level. To be able to perform these behaviors, observed in nature, two scales are playing a crucial role:

- The **timescale** has to be longer than the single-cell action time to allow a broader communication within the system[1];

- The **system dimension** is required to be greater than the single-cell resolution[2] in order to have a collection of individuals able to functionally cooperate and coordinate with one another.

---

[1]For numerical comparison, actin polymerization dynamics, that leads single cell migration, occurs on a timescale of seconds to few minutes [11], resulting in a collective migration on a timescale of tens of minutes, see timing in fig. 1.1.

[2]Reminding that an animal cell is ranging between 10 to $30\mu m$ in length, the system can be composed by 10 to 100 cells, with overall size in the mm.
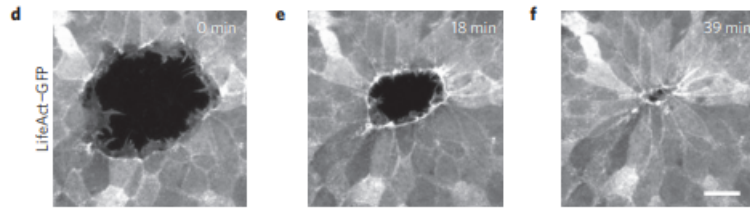
Figure 1.1: *Time course of wound closure in Madin Darby canine kidney cells, adapted from [8]. Images are projections of confocal z-stacks.*
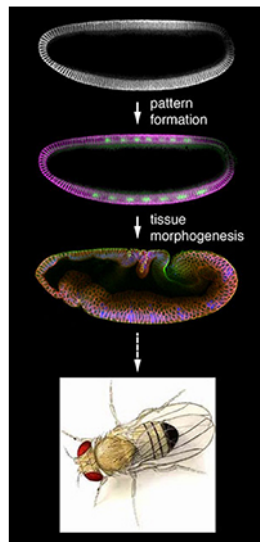
Figure 1.2: *Tissue morphogenesis in Drosophila, from Wang Lab/Epithelial morphogenesis*

Developments in experimental techniques, at these *mesoscale* levels, have uncovered the important role of mechanical interactions between cells [12, 13, 14], that *actively* coordinate the movement, id est *collective migration*, through mechanosensitive adhesion complexes, such as focal adhesion and adherens junctions that can detect and decode physical signaling from the surroundings and coordinate the cellular response[15]. Therefore, tissue and cell mechanics can drive developmental patterning by modifying cell shape and structural integrity, thereby altering cell behavior [16].

Notably, not only are cells able to sense other cells but the coordination happens even through cell-substrate interactions, where the very own physical properties of the substrate[3] such as stiffness, shape, and friction are crucial in determining the outcome [17, 18, 19]. To complicate the picture, a more profound interplay between mechanics and biochemistry has been shown in the coupling of the interactions within cells and substrate [20].

The ability of cells to **convert chemical energy into mechanical forces** is allowing them to do work, both onto the micro-environment and onto neighbors by deformation of the cell interface, while driving the system out of equilibrium in a feedback between shape deformation and active driving [21]. These properties give rise to complex phenomena, not yet fully understood in their detailed form. However, the recent advances described above, have highlighted mechanisms that can be modeled through physical interactions, such as *repulsion* and *adhesion*, and mechanical forces. On this note, it is worth spending a few words regarding interactions:

---

[3]The place where the cells are laid down
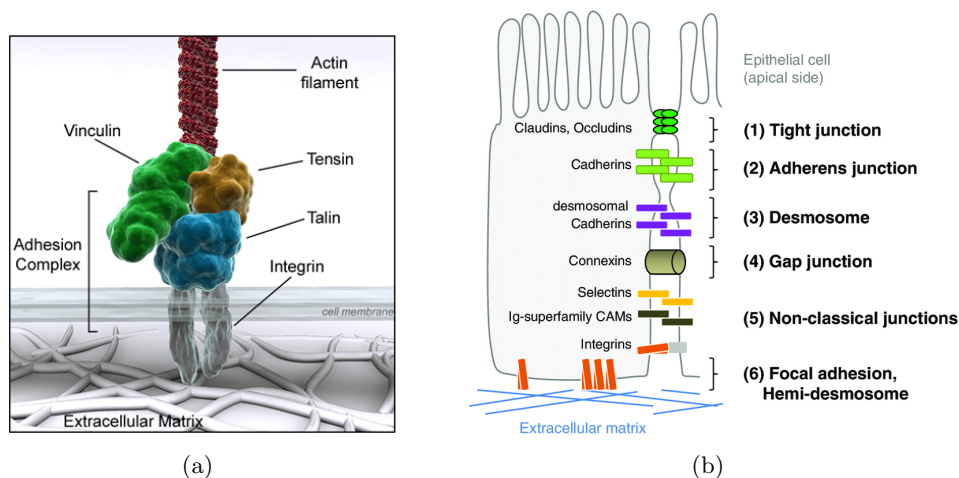
Figure 1.3: *(a)Model of focal adhesion complex, from Nitric Oxide Research group, (b)Diagram of different types of cells adhesion molecules (CAM) in epithelial cells, adapted from [22]*

- **Adhesion**: Cell adhesion is the process by which cells interact and attach to neighboring cells, or extracellular matrix (ECM), through specialized molecules of the cell surface called CAMs, see figure 1.3(b). It should not be regarded as just a *'gluing'* factor, in fact, it can be involved in signal transduction for cells to detect and respond to changes in the surroundings [23, 24] [4], being determinant for the overall architecture of the tissue, and crucial for biological processes such as cell migration [25] and wound healing[26, 27]. Disruptions in adhesion mechanisms, by over- and under-expressing CAMs, cause cell invasiveness and metastasis, for instance by overexpressing integrin [28, 29] a stronger focal adhesion is promoted, id est stronger cell-ECM adhesion, while under-expressing cadherin are allowed to migrate away from the primary cancer source, lowering cell-cell adhesion[23].

- **Repulsion**: Cell repulsion is the dual counterpart of adhesion, arising from the interplay of biochemical and physical signaling, such as electrostatic repulsion [30], mechanical forces like steric repulsion, and downregulation of CAMs. A major role is played in tissue development, where cells actively migrate while pushing or pulling one another in a combination of forces and chemo-repellants[31, 4, 9].
  Notably, a decrease in adhesion does not correspond directly to an increase in repulsion. For instance, there are two major ligand-receptor

---

[4]These transmembrane molecules are able to sense both chemical and physical changes in the environment, such as concentration gradients and substrate stiffness[9]

pairs: Semaphorin-Plexin and ephrin-Eph. Semaphorins act through a complex signaling pathway to inhibit integrin-mediated adhesion, allowing cell repulsion while the second pair, once bonded, induces repulsion or adhesion [32, 33, 34].

In these pages, the aim is to model the mechanics of tissues, through the interactions as explained above, like skin epidermis[5], a real example of a multilayer cellular system. A schematic representation of the skin can be seen in the figure below (Figure 1.4), and from its stratification the reason behind this study, since 3D modeling of tissues is in its infancy and not much is well known.

In this example of a multi-layer cellular system, it is possible to identify different components such as:

- The dermis or *corium* is a layer of skin between the epidermis (with which it makes up the *cutis*) and subcutaneous tissues, and forms the *basement*;

- The *stratum basale* is a single layer of cuboidal basal cells. Some of which can act like stem cells, called *basal keratinocyte stem cells*;

- The rest of the epidermis is composed of differentiated, *daughter*, cells and is divided into three layers, as depicted in the figure 1.4. Thus, forming the *supra-basal layer*
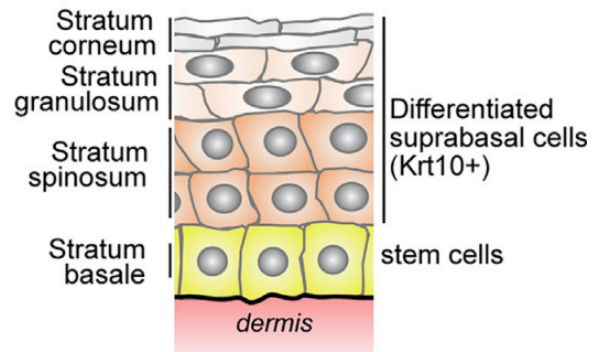
Figure 1.4: *Schematic of the stratified epidermis with basal stem cells and their progeny, differentiated suprabasal cells [35].*

Importantly, different cell layers have different properties, such as different kinds of junctions that lead to different adhesive strengths. The stratum corneum, for instance, presents tight junctions in greater numbers, to provide a physical barrier with the outside. Hereafter, driven by simple principles, these variations are not treated, but a generalization is straightforward.

---

[5]The word epidermis is derived through Latin from Ancient Greek *epidermis*, itself from Ancient Greek *epi* 'over, upon' and *derma* 'skin'

Cells models: an overview

Since the collective dynamics of cellular systems have been observed, the question of how to connect different *scales*, id est single-to.collective behavior, has promoted the formulation of various mathematical and numerical models of cell interactions.

Here, a broad overview of the main concepts behind the major models, represented schematically is shown in the figure 1.5.
A fundamental separation has arisen within the modeling:
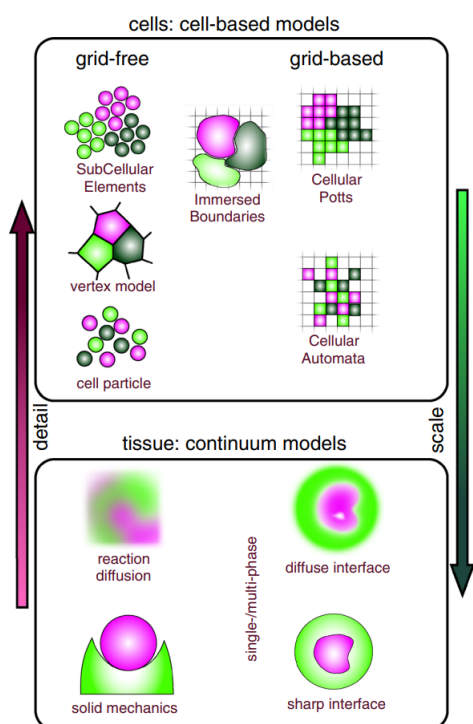
Figure 1.5: *Overview of cell-based and continuum models for biological tissue, from [36]*

- **cell-based models**, also called agent-based models[37, 38], are representing cells as discrete entities, id est agents, and can be further divided into:

  1. Grid-based if cells are initialized on lattice sites;
  2. Grid-free if cells or cells components are initialized as nodes on a network;

  Their advantage lies in the easy integration of single-cell processes in the description of a tissue. A schematic of their differences is given in figure 1.6, on the next page;

- **Continuum models** consider the cells' geometry, accounting for the spatial distribution of both intra- and extracellular processes through solving partial differential equations[39](PDEs) derived from continuum mechanics. This allows the description of systems of cells at a macroscopic level, making the large-scale description of tissue easier thanks to the advent of high-performance computers. These models are approximating cells by a continuum density[40, 41, 42, 43, 44], giving rise to interfaces, both *sharp* and *diffusive*, that are used to distinguish between the various elements of the system; that can be related to phase changes across the borders, therefore allowing the use of **phase field models**.
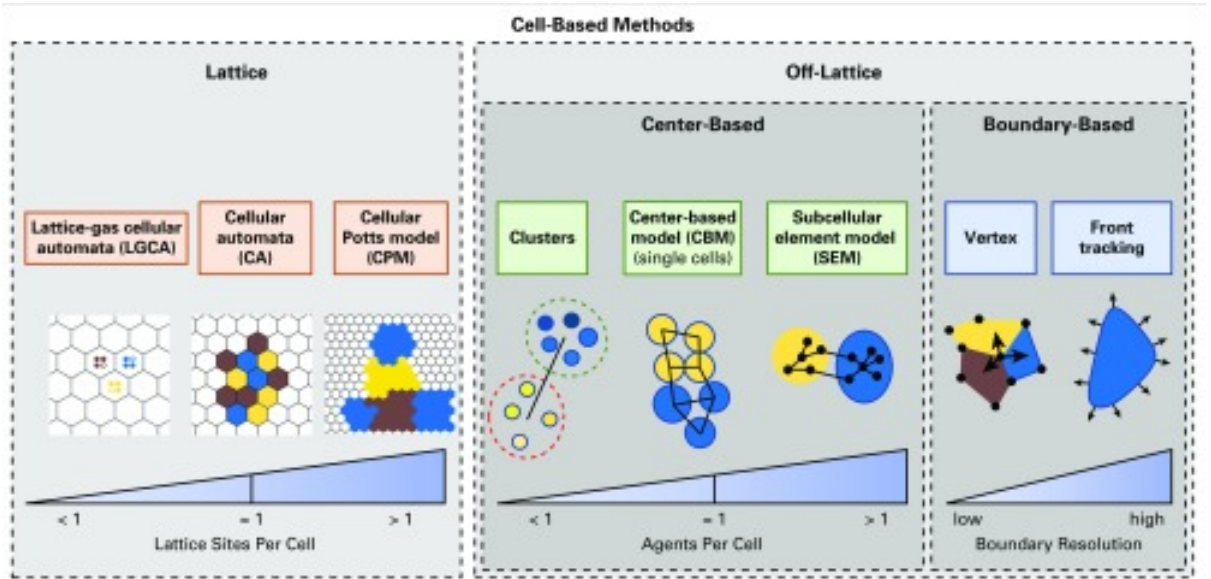
Figure 1.6: *Schematic classification of cell-based models, from [37]*

In this work, a phase field model has been developed to simulate multi-layer cellular systems. A detailed description is given in Methods with here a simple intuition being proposed.

First proposed by Fix[45] and Langer[46] for solidification of binary alloy and for pattern formation in a first-order phase transition, respectively, it is used to model interfacial problems by substituting boundary conditions at the edge with the partial differential equation for the evolution of an auxiliary field, id est the phase-field, that performs as an order parameter[6]. The phase assumes two distinct values, for instance, +1 and -1, in each phase, presence or absence, with a smooth change in between around the interface, which diffuses with a finite width. Therefore any location in the system is defined as the collection of all points where the phase field takes a certain value. In the infinitesimal interface width, the so-called sharp interface, the precise dynamic of it is recovered. The beauty of this method lies in solving PDEs to avoid explicit treatment of the interface's boundary.

Over the last few decades, this idea has been implemented to investigate cells dynamics: from single cell motility[47] to the migration of a few cells[48, 49] as well as for multicellular systems[50, 51, 21, 52, 53] and cell migration[54, 55, 56] but mostly in monolayers, both in two- and three-dimensions. Whereas this study will focus on implementing and modeling multiple layers of cells such as the skin epidermis; adopting as a starting point the results in [21, 53], where the active matter approach is taken into account since tissues have shown to possess liquid crystal features.

---

[6]An order parameter is a measure of the degree of order across the boundaries in a phase transition system

This research aims to clarify the mechanical basis behind stratified cells' behavior, such as the active coordination of their movements through mechanosensitive adhesion complexes, enabling them to move upward or downward while undergoing defined shape changes. Additionally, the study is investigating aspects such as the maintenance of homeostasis and wound healing that have been shown experimentally [35, 57, 58, 16].

The existing tools are inadequate: the interactions between layers of differentiated cells with the basal stem cell layer are happening across multiple stacked layers, and are hardly captured by the present frameworks. Therefore, the extension and modifications on these, above-mentioned, models will fill the existing gap in the knowledge of the mechanics involved in stratified tissues, as well as point out some interesting, not well-known, features such as how multi-layered cellular systems will *actively* become single-layered by collective migration as well as some inherently three-dimensional phenomena like cell extrusion and collective behavior.

By simulating a three-dimensional-multi-layer system, the aim is to explore those intrinsic, fundamental processes of cell biology that require access to both in-plane and out-of-plane forces in the cellular layers and in doing so, to catch up with the experimental techniques, providing them a new tool and breaking the two-dimensional, and semi-three-dimensional, approach used today.

This will provide the foundations for more nuanced theoretical and computational developments, setting a starting point for the understanding of stratified tissues as well as giving a glimpse inside the biological world governed by mechanical forces.

Outline structure

In the following pages, there will be an accurate description of the theoretical background and the mathematical features of the phase field model used, in Methods.
Next in line the results of the simulations will be presented and explained in Results.
Lastly, Conclusion & Outlook will be used to summarize and to provide future developments, starting from this work.

Chapter 2

Methods

Phase field model

A **phase-field model** is a mathematical model for solving interfacial problems, where the phase is the spatial and temporal order parameter defined in a continuum-diffused interface model. With the help of order parameters, many types of complex mesoscale microstructure changes observed in material science are described effectively [59], allowing to approach the evolution of arbitrary morphologies without explicitly tracking the positions of the interfaces.

Over the last few decades, this theory has been applied to many fields ranging from binary alloys [60, 45] to active matter, see [52, 53] for a review. Moreover, cellular systems have displayed features proper of liquid crystals, such as nematic[61, 62, 63, 64, 65, 6, 66] and hexatic[67, 68, 69] order, allowing the use of the mathematical background of phase separation developed to such an extent. Here, a free energy functional is introduced to distinguish into two phases, cell or empty space, and is used for the evolution of the system; an educated guess for a double well potential has led to the Cahn-Hilliard free energy [70].

As for describing the mechanics between the cellular system above, two main interactions have been introduced to mirror the adhesive and repulsive forces between cells in the system. The ability of the cells in converting the energy into work has been introduced in the framework of active soft matter with the help of an active term embedded into the mechanical forces, which has been shown to drive the system out of equilibrium while exhibiting tissue properties [53, 21].

Field evolution

The system consists of two-to-three layers of N spherical cells, stacked one upon the other. Each cell i is modeled as an active deformable droplet through the three-dimensional phase field, $\phi_i = \phi_i(\vec{x})$ and initialized with radius r. The interior and exterior of cell i corresponds to $\phi_i = 1$ and $\phi_i = 0$, respectively, with a diffuse interface of length λ connecting the two regions at the midpoint, $\phi_i = \frac{1}{2}$, delineating the cell boundary.

The dynamics of the phase field ϕ_i is defined through[1]:

$$\partial_t \phi_i + \vec{v} \cdot \vec{\nabla} \phi_i = -\frac{\delta \mathcal{F}_{tot}}{\delta \phi_i}, \quad with \quad i = 1, 2, \cdots, N \tag{2.1}$$

where $\vec{v}_i$ is the velocity of cell i and $\mathcal{F}_{tot}[\phi, \nabla \phi]$ is the three-dimensional free energy functional accounting for cell mechanical properties. The velocity enters Eq.2.1 via the advection term, effectively pushing each cell uniformly as a whole without inducing any deformation of its interface.

A minimal version of the model has been used effectively to describe cell monolayers [52], while a simplified version, not accounting for advection term, has been applied to binary alloys [60, 71].

Here, the total free energy can be separated into two main components, corresponding to the internal ($\mathcal{F}_{int}$) and interaction ($\mathcal{F}_{inter}$) free energy,

$$\mathcal{F}_{tot} = \mathcal{F}_{int} + \mathcal{F}_{inter} \tag{2.2}$$

responding to the interface of the cell and the interaction between both the neighbors and the substrate. The model results from a three-dimensional extension of the two-dimensional free energy functional, described in [72, 73, 49], with additional terms to account for both cell-cell and cell-substrate interactions. The substrate is therefore designed to be a static phase-field ϕ_{sub}, meaning that it will not evolve while interacting with cells.

Internal free energy : $\mathcal{F}_{int}$

Following the steps of [21], a simple set of equations is used to describe the internal mechanical properties of the cell, namely a functional exhibiting two distinct phases (*presence* and *absence* of the cell) and a soft volumetric constraint over the proper volume V_{cell} to make the cell compressible.

$$\mathcal{F}_{int} = \mathcal{F}_{CH} + \mathcal{F}_{vol} \tag{2.3}$$

---

[1]reminding the reader that the functional derivative can be re-written as:

$$\frac{\delta \mathcal{F}}{\delta \phi_i} = \frac{\partial \mathcal{F}}{\partial \phi_i} - \nabla \cdot \frac{\partial \mathcal{F}}{\partial \nabla \phi_i}$$

The internal free energy can be regarded as two parts in Equation 2.3. One is from the Chan-Hilliard free energy, and the other is representing a soft volume constraint energy. Equation 2.4 is the *Cahn-Hilliard free energy*, first introduced in [70], represents a simple formulation exhibiting two distinct phases, as can be seen in Figure 2.1 representing the first term, or *demixing* free energy, corresponding to a double-well potential with the minima at $\phi = 0$ and $\phi = 1$, while the second term is the *mixing* part that penalizes the gradients. The γ here defines the stiffness of the cell[52], and its interface becomes sharper as its width λ goes to zero until approaching a step function, as shown in Figure 2.1 [2], a behavior well approximated by a hyperbolic tangent of size λ.

$$\mathcal{F}_{CH} = \sum_{i=0}^{N} \frac{\gamma}{\lambda} \int d\vec{x} \left\{ 4\phi_i^2(1 - \phi_i)^2 + \lambda^2(\nabla\phi_i)^2 \right\} \tag{2.4}$$
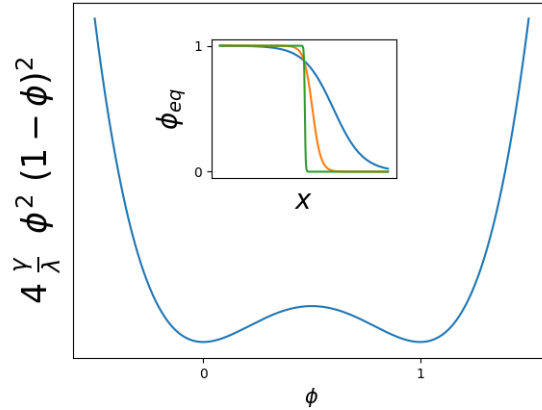
Figure 2.1: ***Interfacial profile for** ϕ: The double-well potential corresponding to the demixing free-energy, Cahn-Hilliard free-energy in eq. 2.4. The inset shows the equilibrium phase field profile for different values of λ, where a sharp interface is obtained for $\lambda \to 0$*

Equation 2.5 provides a soft constraint for the cell volume (relation 2.6, where r is the cell radius), accounting for deformability of cells through the compressibility μ, enforcing the constraint around the proper volume, where in the absence of any form of adhesion, neither cell-cell nor cell-ECM, the cells

---

[2]Refer to [52] for the equilibrium phase ϕ_{eq}

will relax into spheres of radius r, providing a large domain [74].

$$\mathcal{F}_{vol} = \sum_{i}^{N} \mu \left\{ 1 - \frac{1}{V_{cell}} \int d\vec{x} \phi_i^2 \right\}^2 \tag{2.5}$$

$$\text{where :} \quad V_{cell} = \frac{4}{3} \pi r^3 \tag{2.6}$$

The required behavior is then described through the square potential of strength μ ensuring the volumes of the cells $V_i = \int d\vec{x}\phi_i^2$ are close to $\frac{4}{3}\pi r^3$, penalizing higher deviations from the proper value V_{cell} [3].

Interaction free energy : $\mathcal{F}_{inter}$

In this paragraph, a broad and intuitive explanation of the interaction term is given and the nuance in the model is introduced: **the cell-substrate interaction**, by the most recent work described in [53].

While most previous work on the same model [21, 52] has dealt with interactions by reducing them to the cell-cell repulsion term in equation 2.9, here even the cell-cell adhesion has been taken into consideration, in the form shown in equation 2.10, as well as a parallel set of equations (Eq. 2.13, 2.12) for the interactions with the substrate, represented by a new, independent, phase-field ϕ_{sub}.

$$\mathcal{F}_{inter} = \mathcal{F}_{rep} + \mathcal{F}_{adh} \tag{2.7}$$
$$\mathcal{F}_{adh(rep)} = \mathcal{F}_{adh(rep)}^{cc} + \mathcal{F}_{adh(rep)}^{cs} \tag{2.8}$$

As shown in the above equations, the interaction free energy has been initially divided into two major components, namely $\mathcal{F}_{adh}$ and $\mathcal{F}_{rep}$ representing adhesion and repulsion potential, respectively. The superscript cc is referring to cell-cell, and cs to cell-substrate free energy. It is worth noting that the two components, to be consistent, have to carry different signs, id est, positive $(+)$ for repulsion and negative $(-)$ for adhesion; since the first provides *'more'* freedom to the cell, in the form of allowing more deformations and easier movement, while the second binds the system to a more compact state.

A further division in each of the components just described has been carried over, allowing a better understanding of the interactions that come into play, for instance in the equation 2.8 it can be seen that for both adhesion and repulsion, two main characteristics are considered: cell-cell and cell-substrate.

Moreover, the free energy comprises gradient contributions $(\vec{\nabla}\phi)$ accounting for, and distinguishing between, cell-cell (ω_{cc}) and cell-substrate (ω_{cs}) adhesion as well as cell-cell (κ_{cc}) and cell-substrate (κ_{cs}) repulsion [53] in the following way:

---

[3]The volume is proportional to the square to ensure that it is *always* positive even when the phase field is slightly negative which can happen during simulations [52]

cell-cell interactions

The formulation has been created for simplicity's sake. Nonetheless, it captures the main features of a multicellular system such as:

- Cell-cell repulsion, defined in equation 2.9, which penalizes regions where two or more cells overlap through an energy scale $\frac{\kappa_{cc}}{\lambda}$[4]. This term intuitively represents the capabilities of the cells to maintain intercellular space as well as the inability to compenetrate one another;

- Cell-cell adhesion, defined in equation 2.10, which by promoting adhesion between the cells, it reduces the degrees of freedom of the system making the core of the system more compact through an energy scale $\frac{\omega_{cc}}{\lambda}$ [4]. Therefore representing the ability to tightly connect neighbors through junctions and cooperation.

$$\mathcal{F}_{rep}^{cc} = \sum_{i}^{N} \sum_{j \neq i} \frac{\kappa_{cc}}{\lambda} \int d\vec{x} \phi_i^2 \phi_j^2 \tag{2.9}$$

$$\mathcal{F}_{adh}^{cc} = \sum_{i}^{N} \sum_{j \neq i} \frac{\omega_{cc}}{\lambda^2} \int d\vec{x} \nabla \phi_i \cdot \nabla \phi_j \tag{2.10}$$

In the above formulation it can be noted that the repulsion is applied across the cell interface, the surface that encloses the cell's volume, as can be seen by a comparison with the soft volumetric constraint where $\int d\vec{x} \phi_i^2$ also appears. While the adhesion comprises a more complex behavior due to the presence of the gradients $(\nabla \phi_i)$ that allow it to act even within the cell volume.

To improve the numerical stability, a **new** formulation of the cell-cell adhesion has been introduced below(Equation 2.11). The detailed derivation of the functional derivative is given in Appendix: New cell-cell adhesion and example of calculation.

$$\mathcal{F}_{adh}^{cc} = \sum_{i}^{N} \sum_{j \neq i} \omega_{cc} \lambda \int d\vec{x} (\nabla \phi_i)^2 \cdot (\nabla \phi_j)^2 \tag{2.11}$$

.

---

[4]with units of volumetric energy density, id est energy/volume

cell-substrate interactions

$$\mathcal{F}_{rep}^{cs} = \sum_i^N \frac{\kappa_{cs}}{\lambda} \int d\vec{x} \phi_i^2 \phi_{sub}^2 \qquad (2.12)$$

$$\mathcal{F}_{adh}^{cs} = \sum_i^N \frac{\omega_{cs}}{\lambda^2} \int d\vec{x} \nabla \phi_i \cdot \nabla \phi_{sub} \qquad (2.13)$$

However, in nature, the dynamic of clustered cells does not happen in empty spaces [5], but rather it requires a scaffold to provide the optimal microenvironment for seeded cells: either synthetic or natural, like the protein network of the extracellular matrix (ECM). This scaffold, here called more generally *substrate*, helps cells attach to, and communicate with, nearby cells, and plays an important role in cell growth, cell movement, and other cell functions like coordinated motion and protrusion formation.

Therefore, it is natural and reasonable to include an environmental component in the model. Driven by the same simplicity principles followed so far, and in accordance with [53], a static phase-field, representing the substrate, has been introduced, namely ϕ_{sub} representing a non-trivial boundary, such as a wall [52, 75].

Note that its phase is defined to be an additional, different phase from the cellular phases; while preserving the same overall idea, id est $\phi_{sub} = 1$ for the *presence* of the substrate and $\phi_{sub} = 0$ for its *absence*; while $\phi_{sub} = 0.5$ for its boundary. At the same time the substrate is *static* meaning that, once defined, it does not evolve and maintains the same shape.

Here, by any loss of generality, the substrate is introduced as a rectangular parallelepiped spanning the whole xy-plain, while having a smaller depth[6], in order to avoid edge effects[7], and the cells are laid on top of it.

The cell-substrate interaction is carried over with the cells that are in contact with, or close enough to the substrate (within a distance $d_{inter} \approx 2r_{cell}$) according to the equations 2.12, 2.13; it has to be noted they form a complementary set to eq. 2.9, 2.10 where $\sum_{j \neq i}$ has been removed since $\phi_{sub} \neq \phi_i \in \phi_{cell}$ by definition.

---

[5]During the last five years the development of cells has been studied on the International Space Station in a microgravity environment, and even then a supporting extracellular matrix has been used, known as tissue chips. For reference NASA: Organs-On-Chips

[6]$height(z) \ll lenght(x), width(y)$

[7]In such way that cells will not reach the edge of the substrate

Two main features are represented by the above set of equations:

- Cell-substrate repulsion, defined in equation 2.12, which penalizes regions where cells overlap with the substrate through an energy scale $\frac{\kappa_{cs}}{\lambda}$ [4]. Intuitively, the repulsive effect, avoiding compenetration, allows the formation of single-cell protrusions over the surface while reducing cell-cell coupling [76].

- Cell-substrate adhesion, defined in equation 2.13, which by promoting adhesion between the cells and substrate, reduces the degree of freedom of the system by an anchoring effect through an energy scale $\frac{\omega_{cs}}{\lambda}$ [4]. Cells that are adherent to a surface may coordinate their motion with neighboring cells through protrusion waves that travel across cell-cell contacts [76], hence allowing collective behavior.

The complex interplay between cells and substrate involves a plethora of phenomena that can be divided into two main categories: **substrate-mediated cell response** and **cell-mediated substrate remodeling**[77]. The focus of this work has been set over the first one[8], which comprehends cell proliferation[9], differentiation[9], and spreading with the formation of the above-mentioned protrusions.

---

[8]The latter comprises synthesis, recruitment, and degradation of the extracellular matrix
[9]Not yet included into the model

Dynamics

The velocity $\vec{v}_i$, of each cell can be obtained from a force balance equation: since Reynolds numbers are typically low ($Re \sim 10^{-4}$) for cell monolayers [78, 52], and an educated guess ($Re \ll 1$) has been made for multilayer systems[10], the following overdamped dynamic can be assumed [79]:

$$\xi\vec{v}_i = \vec{F}_i^{total} = \vec{F}_i^{act} + \vec{F}_i^{inter} \tag{2.14}$$

Here, ξ is the substrate friction coefficient and $\vec{F}_i^{total}$ is the total force acting on the interface of cell i [75, 21].

The exact definition of the total force can be changed accordingly to the model to include different contributions arising from different sources such as interactions with other cells or substrates ($\vec{F}_i^{inter}$), and active forces ($\vec{F}_i^{act}$) due to the intrinsic activity of the cells that drives the system out of equilibrium[11]. Following [75, 21, 53, 52], the microscopic interface forces can be modeled using a macroscopic tissue stress tensor, σ_{tissue} according to:

$$\vec{F}_i^{total} = \int d\vec{x}\phi_i\vec{\nabla} \cdot \sigma_{tissue} \tag{2.15}$$

$$= -\int d\vec{x}\sigma_{tissue} \cdot \vec{\nabla}\phi_i \tag{2.16}$$

Equation 2.15 is representing the integral of the local force weighted by the phase field ϕ_i, while equation 2.16 is the integral of the force exerted by the stress tensor on the vector $-\vec{\nabla}\phi_i$ normal to the interface and pointing outwards [21][12].

The above equations are used to connect the local properties of single cells to the overall properties of the tissue; noticing that, in the limit of sharp interface (id est $\lambda \to 0$), eq. 2.16 tends to a contour integral over the surface encompassing the cell volume [75].

---

[10]Reminding

$$Re = \frac{\rho v_i L}{\mu'}$$

where

- ρ is the density,
- μ' is the dynamic viscosity,
- v_i is the flow speed,
- L is the characteristic linear dimension;

it is reasonable to extend the monolayer magnitude of Re to multilayers since the only thing that changes is the height of the system

[11]Honorable mention to another possible component, the polar driving forces described in [53, 52]

[12]The derivation from eq 2.15 to eq 2.16 can be done through the divergence theorem:

$$\int\int\int d\vec{x}\vec{\nabla} \cdot \sigma = \int\int d\vec{x}\sigma \cdot \vec{n}, \text{ with } \vec{n} = -\vec{\nabla}\phi$$

Stresses

In analogy to continuum theories, the stress tensor can be separated into *passive* and *active* components, to account for extensile characteristics such as cell extension and alignment [80], in the following fashion:

$$\sigma_{tissue} = -\mathcal{P}I - \zeta\mathcal{Q} \tag{2.17}$$

where $\mathcal{P}$ is the tissue pressure field, $\mathcal{Q}$ is the tissue nematic tensor and I is the identity tensor while ζ quantifies the intensity of the field. More precisely, the following relations have been used:

$$\mathcal{P} = \sum_i^N \frac{\delta\mathcal{F}_{tot}}{\delta\phi_i} = \sum_i^N \left(\frac{\delta\mathcal{F}_{inter}}{\delta\phi_i} - \frac{\delta\mathcal{F}_{int}}{\delta\phi_i} \right) \tag{2.18}$$

$$= \sum_i^N \left(\frac{\delta\mathcal{F}_{rep}}{\delta\phi_i} + \frac{\delta\mathcal{F}_{adh}}{\delta\phi_i} - \frac{\delta\mathcal{F}_{CH}}{\delta\phi_i} - \frac{\delta\mathcal{F}_{vol}}{\delta\phi_i} \right) \tag{2.19}$$

$$\mathcal{Q} = \sum_i^N \phi_i\mathcal{S}_i \tag{2.20}$$

$$\mathcal{S}_i \equiv -\int d\vec{x} \left\{ (\nabla\phi_i)^T\nabla\phi_i - \frac{1}{3}Tr\{(\nabla\phi_i)^T\nabla\phi_i\} \right\} \tag{2.21}$$

where $\mathcal{S}_i$ is the deformation tensor of cell i [81] defined as above[13], with its eigenvalues and eigenvectors measuring the strength and orientation of the main deformation axes of the cell. To ensure that $\mathcal{Q}$ is defined at each point in space, the multiplication by the phase field is carried over.

By using equation 2.18, as noted in [49], provides much freedom in the definition of the pressure field, which represents a simple elastic repulsion force between cells.

The second term in the right-hand side of equation 2.17 is introduced to provide a local active term, related to the deformation of cells via eq 2.20, capable of driving the system out of equilibrium and to capture the active nematic phenomenology of cells in analogy with active liquid crystals [75, 21, 5, 64]; that can be interpreted as dipolar force density distributed along the cell interfaces, resulting in each cell pushing or pulling its neighbors depending on the direction of their contact area with respect to the stress tensor[52, 21].

---

[13]The traceless part of $-\int d\vec{x}(\nabla\phi_i)^T\nabla\phi_i$

Gathering everything up, the dynamic of the system can be described as follows:

$$\xi\vec{v}_i = \vec{F}_i^{total}$$

$$= -\int d\vec{x}\sigma_{tissue}\cdot\vec{\nabla}\phi_i$$

$$= -\int d\vec{x}(-\mathcal{P}I - \zeta\mathcal{Q})\cdot\vec{\nabla}\phi_i$$

$$= \int d\vec{x}(\mathcal{P}I)\cdot\vec{\nabla}\phi_i + \int d\vec{x}(\zeta\mathcal{Q})\cdot\vec{\nabla}\phi_i$$

$$= \int d\vec{x}\{\sum_i^N(\frac{\delta\mathcal{F}_{rep}}{\delta\phi_i} + \frac{\delta\mathcal{F}_{adh}}{\delta\phi_i} - \frac{\delta\mathcal{F}_{CH}}{\delta\phi_i} - \frac{\delta\mathcal{F}_{vol}}{\delta\phi_i})I\}\cdot\vec{\nabla}\phi_i + \int d\vec{x}\{\zeta\sum_i^N\phi_i\mathcal{S}_i\}\cdot\vec{\nabla}\phi_i$$

$$= \vec{F}_i^{inter} + \vec{F}_i^{act}$$

Leading to:

$$\vec{F}_i^{inter} = \int d\vec{x}\{\sum_i^N(\frac{\delta\mathcal{F}_{rep}}{\delta\phi_i} + \frac{\delta\mathcal{F}_{adh}}{\delta\phi_i} - \frac{\delta\mathcal{F}_{CH}}{\delta\phi_i} - \frac{\delta\mathcal{F}_{vol}}{\delta\phi_i})I\}\cdot\vec{\nabla}\phi_i \qquad (2.22)$$

$$\vec{F}_i^{act} = \int d\vec{x}\{\zeta\sum_i^N\phi_i\mathcal{S}_i\}\cdot\vec{\nabla}\phi_i \qquad (2.23)$$

Numerical implementation

In this section, a broad overview of the implementation is given. The aim is to understand the mechanics of a multi-layer cellular system with a focus on the features that allow it to become a mono-layer in a process known as morphogenesis. Each cell is modeled as an active deformable droplet. For instance, the cells under examination may be epithelial cells and the substrate may be viewed as the extracellular matrix (ECM).

To do so, each cell's center is initialized on a cubic lattice[14], at position $\vec{x}$, via a Poisson sampling[15] inside the chosen volume at given heights to form layers; to avoid overlapping cells the sampling volume has been decomposed into independent components, namely a 2D xy-surface, where the actual sampling takes place and fixed values of the z-axis according to: $\mathbb{R}^3 = \mathbb{R}^2 \times \mathbb{R}^1$.

Moreover, to each center has been added the cell's radius ($r = 8$, in lattice units) in every direction to successfully build a spheroid with volume $V_{cell} = \frac{4}{3}\pi r^3$. To each lattice point $p_{latt} = (x_{latt}, y_{latt}, z_{latt})$ and for each cell, a phase field $\phi_i^{cell}(\vec{x}) = \phi_i$ is assigned [16], where the usual initialization is used:

- $\phi_i = 1 \; if \; p_{latt} \in V_{cell}$, for cells;

- $\phi_i = 0 \; if \; p_{latt} \notin V_{cell}$, for empty space.

Since the cells are placed over a substrate, a second field is initialized, $\phi_i^{substrate}(\vec{x}) = \phi_i^s$; that forms a rectangular box underneath the cells, which spans the whole xy-plain and has a thickness of about one cell's radius, in order to avoid interactions with the edges. The same substrate field is used to build a cubic box that surrounds the cells in the initialization process, after which it is removed letting the cells free from the constraint.

Note that, for simplicity and without loss of generality, it is considered that cell-substrate interactions take place solely between the bottom substrate and the adjacent cells, and any further generalization is straightforward. During initialization, the system is set as *"passive"*, meaning that no activity ($\zeta = 0$) is involved and therefore the cells are only allowed to reorganize themselves. Providing the system with enough time to settle during a passive, bounded by cubic substrate, state, allows proper initialization resulting in more consistent and biologically relevant results.

The follow-up process consists of a passive mode where the cells are free to expand; while previously the bounded system strongly inhibits the growth.

---

[14]Considering lattice step-size to be 1 in arbitrary units

[15]Taking into account the required spacing between cells, id est at least spaced by the cell radius

[16]For numerical implementation the assigned field is as big as the whole system volume: (*length * width * height*)

Evolution and Tools

The implementation of the evolution of the phase field, as described in Methods: Field evolution, can be described as follows:
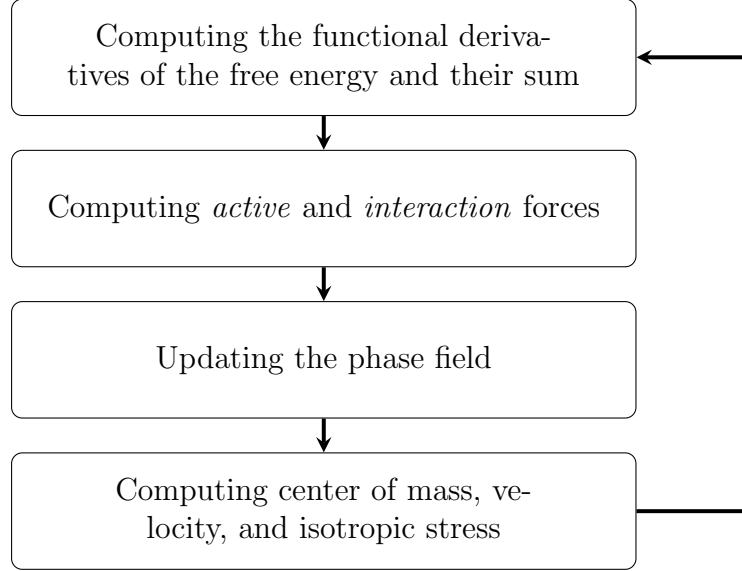
Figure 2.2: *Flowchart for the simulations*

More precisely, the derivatives of the phase field are computed with the usual finite difference method using the central difference formula[17], while an example of computation of the functional derivative of free energy is given in the Appendix: New cell-cell adhesion and example of calculation. The evaluation of the sum of all the free energy terms is carried over according to the pressure definition in equation 2.19, and a first update of the field is done for the simple *passive* system ($\zeta = 0$) by multiplying the result for the time increment dt, since from equation 2.1:

$$\frac{d\phi_i(t)}{dt} = -\frac{\delta\mathcal{F}_{tot}}{\delta\phi_i} - \vec{v}_i \cdot \nabla\phi_i \tag{2.24}$$

$$\Rightarrow \phi_i(t) = \phi_i(t-1) + d\phi_i(t) \tag{2.25}$$

$$where : \ d\phi_i(t) = -\left\{ \sum_i \frac{\delta\mathcal{F}}{\delta\phi_i} + \vec{v}_i \cdot \nabla\phi_i \right\} * dt \tag{2.26}$$

---

[17]In the simple case:

$$\frac{\partial\phi_i(\vec{x})}{\partial x} = \frac{\phi_{i+1} - \phi_{i-1}}{2}$$
$$\frac{\partial^2\phi_i(\vec{x})}{\partial x^2} = \frac{\phi_{i+1} - 2\phi_i + \phi_{i-1}}{4}$$

where i is the lattice node number

Where the second term in the right-hand side of the equation 2.24 is present if the system is considered *active*, namely $\zeta \neq 0$.

To analyze the system behavior, the following feature have been extracted from the phase field evolution:

☞ **Center of mass**: The center of mass has been evaluated by the usual discrete definition, namely:

$$\mathbf{X}_i = \frac{\sum_i m_i \vec{x}_i}{\sum_i m_i}$$

where each position $\vec{x}_i$ corresponds to a lattice point, and the masses m_i are represented by the value assumed by a boolean masked phase field ($\phi_i > 0.5$) at the given points. In other words, 1 or 0 if the value of ϕ_i at one point satisfies the masking criteria, id est *inside* or *outside* the cell.

☞ **Velocity**: First of all, a distinction has to be made between the total velocity of the i-th cell $\vec{v}_i$ and the tissue velocity $\mathbf{V}$:

$$\vec{v}_i = \frac{\vec{F}_i^{total}}{\xi} \ and \ \mathbf{V} = \sum_i \phi_i \vec{v}_i,$$

where the individual velocity is used to analyze single-cell movements and is referred to the center of mass, coming from 2.14, while the latter is giving a more broad idea of the flow of the system.

☞ **Isotropic stress**: To better understand the evolution of a multi-cellular system, as described in the section Dynamics, the tissue stress tensor σ_{tissue} has been analyzed by calculating its *trace*, known as isotropic stress tensor:

$$\sigma^{iso} = \frac{1}{3} Tr(\sigma_{tissue}) \Rightarrow \begin{cases} \sigma^{iso} > 0 \ for \ expansion \\ \sigma^{iso} < 0 \ for \ compression \end{cases}$$

representing the diagonal elements, comprising the tissue pressure as well as the shape deformations according to the equation 2.17. Note that the main components of the trace σ_{ii} roughly represent the *principal stresses* in the Cauchy stress tensor, giving an idea of the direction and the intensity of the stress applied to the main surfaces.

☞ **Coordination number**: The number of neighbors of each cell in the system has been taken into account to provide another indication of the formation of a monolayer, that in a hexagonal close-pack symmetry is 6, from a multilayer, where in the same symmetry provide a variable number from 9 (for the bottom layer) to 12 (for a middle layer). Note that the evaluation of a neighbor is computed within a cell diameter from each cell center, for instance
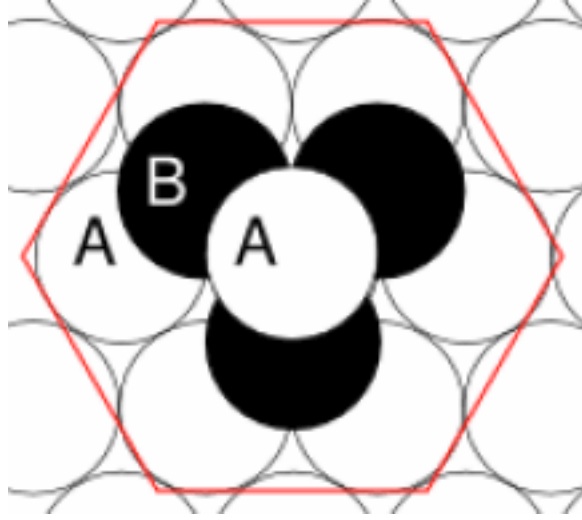
Figure 2.3: ***Example of hexagonal close pack symmetry:*** *A is the bottom layer, B is the top layer*

The vast majority of the model has been done using Python 3.10 and has run both locally and on the High-Performance Computer at the University of Copenhagen. The visualization of the system has been done using both Matplotlib[18] and Paraview[19]. The data analysis has been carried over with Python and Matlab[20].

Parameters

In this section, a general view of the parameters used in the simulations will be given. Note that, the parameters *per se* have to be considered as a set of unitless values that allow the simulations to be carried over without any numerical instability, and any real-life comparison has to be handled with kid gloves. For a better understanding of the scales involved, the magnitude of the units involved is presented in Table 2.1, alongside the values used for the implementation.

Moreover, in this section, a set of re-scaled parameters is presented to ideally allow a broad comparison between the experiments and the simulations. The idea is to use the well-known dimensionality of physical properties such as force, velocity, energy, length, and time to obtain dimensionless numbers through dimensional analysis, even when it means assigning different dimensions to the parameters such as friction, that is notoriously dimensionless[21].

---

[18]For a fast visualization based on a triangular-surface plot of the cells

[19]For visualization of the system with isotropic stresses and tissue velocity

[20]For publication quality plot, PubPlot

[21]In fact, usually $dim(\xi) = 1$, but here is assumed overdamped dynamics, meaning that

$$dim(\xi \vec{v}_i) = dim(\vec{F}_i) \Rightarrow dim(\xi)\frac{L}{T} = \frac{ML}{T^2} \Rightarrow dim(\xi) = \frac{M}{T}$$

This nondimensionalization is used to reduce the number of dimensional variables in any equation into a smaller set of dimensionless parameters in accordance with Rayleigh's method of dimensional analysis and its formal counterpart: the Buckingham π theorem. As can be noticed from Table 2.2, the actual set of parameters used is (γ, ξ, R_0), and from their combination is possible to re-scale every other variable such as $(\sigma, \omega, \vec{v}_i, t, len, \kappa)$.

Following [53], to focus on the interplay of cell-cell and cell-substrate adhesion strengths, the following set of cell-substrate adhesion has been selected: $\omega_{cs} \in \{0.0015, 0.002, 0.0025, 0.003, 0.015, 0.02\}$ while cell-cell adhesion coefficients are mainly set by $\Omega = \frac{\omega_{cc}}{\omega_{cs}} \in \{0.1, 0.5, 0.7, 1, 2, 3, 4, 5, 10, 20\}$ according to the different cases.
As discussed above, the initialization time is fundamental for coherence and consistency and the initialization steps are set to be $n_{init} \in \{1000, 2000, 3000\}$, and the overall simulations are carried over with $n_{sim} \in \{2000, 4000, 6000\}$ steps.

Simulation Parameters			
Meaning	Symbol	Value	Units
Elasticity	γ	0.025	$\frac{N}{m}$
Interface width	λ	3.5	μm
Compressibility	μ	10	$\frac{m^2}{N}$
Substrate friction	ξ	10	$\frac{Kg}{s}$
Radius	r	8	μm
Box size	L_x, L_y, L_z	150, 150, 50	μm
Time increment	dt	0.1	s
Adhesion	ω		
Repulsion	κ		

Table 2.1: *Example and order of magnitude of parameters used in simulations*

Re-scaling Factors				
Meaning	Symbol	Value	Units	Re-scaling use
Elasticity	γ	0.025	$\frac{N}{m}$	Adhesion Coefficient
Characteristic velocity	$\nu = \frac{R_0}{\tau}$	0.02	$\frac{m}{s}$	Velocity
Characteristic stress	$\varsigma = \frac{\gamma}{R_0}$	0.003	$\frac{N}{m^{2]}}$	Stress components
Characteristic size	R_0	8	μm	Lengths
Characteristic time	$\tau = \frac{\xi}{\gamma}$	400	s	Time

Table 2.2: *Re-scaling factors used during analysis*

---

where M = mass, L = length, and T = time

Re-scaled Parameters		
Meaning	Symbol	Value
Length	$\frac{len}{R_0}$	
Time	$d\tau = \frac{dt}{\tau}$	0.00025
Velocity	$\frac{v}{\nu}$	
Stress	$\frac{\sigma}{\varsigma}$	
Adhesion	$\frac{\omega}{\gamma}$	

Table 2.3: *Example of re-scaled parameters used in data analysis*

Chapter 3

Results

In this chapter, the results of the simulations based on the numerical implementation are presented. Two systems are examined :

1. A **two-layer** cellular system with analysis based on the *overall* behavior using mainly averages over all its components and with the focus on *when* it is developing into a monolayer;

2. A **one-layer** system with analysis based on the behavior of the *neighbors'* mechanical properties that allow a single cell in the upper layer to merge into a confluent layer, followed by a focus on how it is happening.

Even if the two systems are conceptually similar, from an implementation standpoint they differ in the order of magnitude of the parameters required to make it stable and biologically relevant. Considering that the cells cannot compenetrate one another, the activity required for the formation of a monolayer in the first system might result greater than in the latter if we compare the timescales. Moreover, the same is valid for adhesion which has to be greater to avoid cell scattering, resulting in a higher 'barrier' to overcome for the cells to detach and merge into one layer.
Nonetheless, the resulting phenomenon is the same, and with this in mind, it is possible to make qualitative comparisons between the two, allowing a clearer understanding of the mechanical basis that is behind the morphogenesis.

Multi-layers

To understand the behavior of multi-layer cellular systems, at first, a second active layer of cells is added on top of a single layer that is located over a solid substrate. To effectively capture the properties behind the morphogenesis, the center of mass (COM) is tracked and to it, velocities, stresses and a number of neighbors are assigned according to the definitions presented in the previous chapter: Methods. In figure 3.1 a two-layer system is represented composed

(a) t=0   (b) t=1.25 τ (c) t=2.5 τ
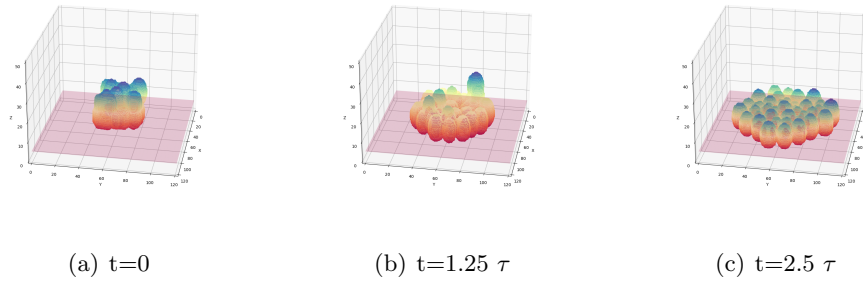
Figure 3.1: *Example of a high activity system, id est $\omega_{cc} = 1.2$, $\omega_{cs} = 0.6$, $\zeta = 3.2$, where 44 cells are forming a monolayer starting from a two layer system. In transparent red is the top layer of the substrate, color are representative of the relative height of the system.*

of 22 cells per layer, that is evolving into a compact monolayer, thanks to the strong cell-cell adhesion, on a short timescale due to the high value of activity.

The same behavior is common to all confluent systems in this study: from a compact system at the end of the initialization, as in figure 3.1(a), the lower cells have to spread to create space for the allocation of the upper layer's cells that meanwhile are expanding, see upper cell in figure 3.1(b) that is bigger than it previously was. Once some space is created the above cells are starting to fill the gaps left by the motion of the lower ones to finally form a confluent monolayer, as shown in figure 3.1(c). This process can be better understood by looking at the three-dimensional trajectories, the two main examples of formation and not formation of a single layer are shown in figure 3.2(a) and 3.2(b), respectively.
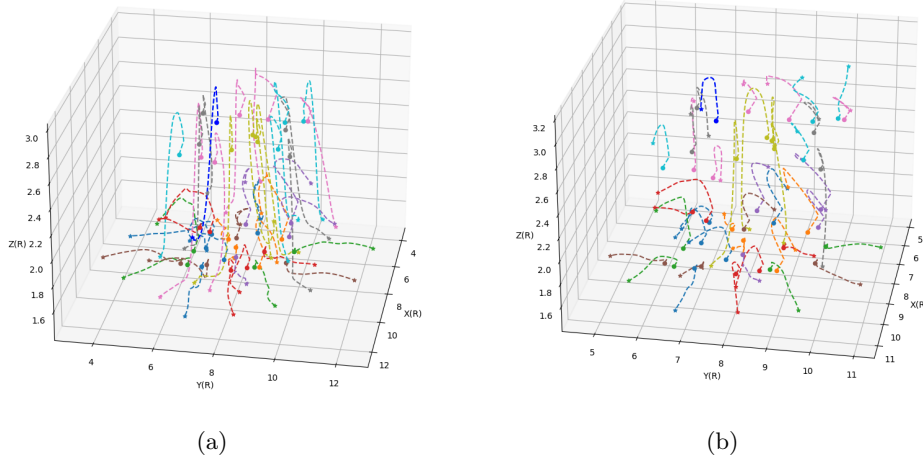
Trajectories

During either the formation of a single layer or the stabilization of a multi-layer, it is noticeable that firstly the COMs of the upper layer are rising which is representing the cells' growth: in fact, since the cells' growth is simultaneous, two major components are at the base of the phenomenon, namely (1) cell volume is increasing homogeneously in all directions, slightly moving to their center, It is more noticeable if we focus on the lower layer of figure 3.2(b); and

(2) the stacked layer is being pushed upwards even more in response to the growth, this is clearer in figure 3.2(a).

Once the activity kicks in and the cells move away from each other, in one case the above ones fill the lower gaps, represented by the straight vertical lines in figure 3.2(a) allowing the formation of a single layer; while in the other scenario, when the activity is low, they tend to stabilize on the upper layer, depicted by short and convoluted lines as in figure 3.2(b).
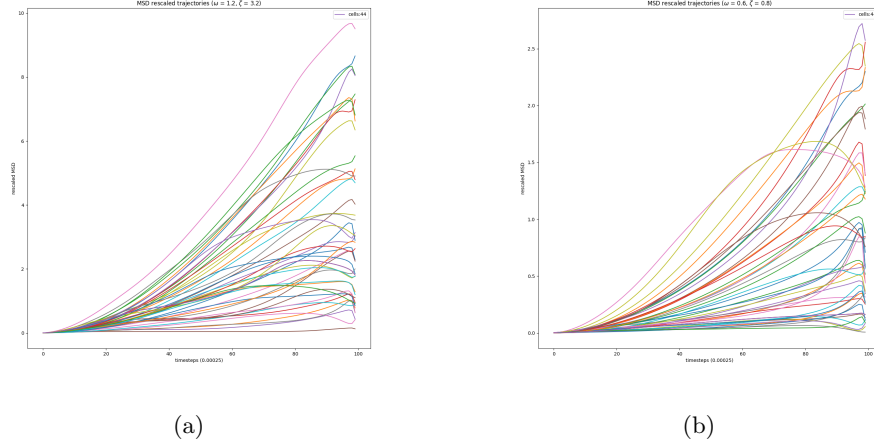

(a)   (b)

Figure 3.2: *Example of a 3D trajectory tracking of the center of mass of each cell in the two different scenarios: (a) Formation of a monolayer with $\omega_{cc} = 1.2$, $\omega_{cs} = 0.6$, $\zeta = 3.2$, and (b) Activity in a two layers system, not forming a monolayer with $\omega_{cc} = 0.6$, $\omega_{cs} = 0.6$, $\zeta = 0.8$. The dots are the initial positions, the stars are the final positions and the dashed lines represent the time evolution of the trajectories.*

Therefore, during the evolution of the system, two main types of motion are arising:

☞ The lower layer is expanding in contact with the scaffold due to the interaction with the substrate. This happens radially outwards from their initialized positions due to cell growth. The inflation pushes one another away and increases the height of their center of mass since they cannot expand below the substrate. Moreover, once the activity is introduced, it drives cells to a stable configuration where the free energy is minimized.

☞ The upper layer, not in contact with the substrate experiences the same growth plus the initial push from below; while after gaps are created their motion is linear and vertical due to activity and cell-cell adhesion that are driving the system in a stable state and binding the cells to form a confluent layer, respectively.

Mean Squared Displacement

These two aspects are better captured by the Mean Squared Displacement (MSD) of the system[1]

(a)   (b)

Figure 3.3: *Example of a Mean Square Displacement (MSD) of the center of mass of each cell in the two different scenarios: (a) Formation of a monolayer with $\omega_{cc} = 1.2$, $\omega_{cs} = 0.6$, $\zeta = 3.2$, and (b) Activity in a two layers system, not forming a monolayer with $\omega_{cc} = 0.6$, $\omega_{cs} = 0.6$, $\zeta = 0.8$.*

In figure 3.3, both scenarios are depicted, clearly distinguishing two different types of motion based on the activity of the system and on the initial height of the cell as can be seen from the two types of curves and their final values. In fact, in figure 3.3(a), with high ζ, the system is dominated by activity, and for greater values of MSD the shape corresponds to direct motion, representing the top layer; instead, the lower final MSD values are initially pushed by activity and then reach a maximum value that drops before the final time, representing the lower layer whose cells form a configuration with gaps in between and diffuse afterward, since they basically get confined by adhesion, while a monolayer is formed.

On the other hand, in figure 3.3(b), for low values of ζ, the cells are still driven by activity at first, but the system is *'frozen'* by adhesion further along giving rise to a diffusive motion that does not allow the same amount of gaps to form in the lower layer; the fact that there are greater values of MSD is an indication that more cells from the top layer are not being incorporated into the one below.

---

[1]The MSD is measured over time, in biophysics, to determine if a particle is spreading slowly due to diffusion, or if an advective force is also contributing, referring to figure 3.4.
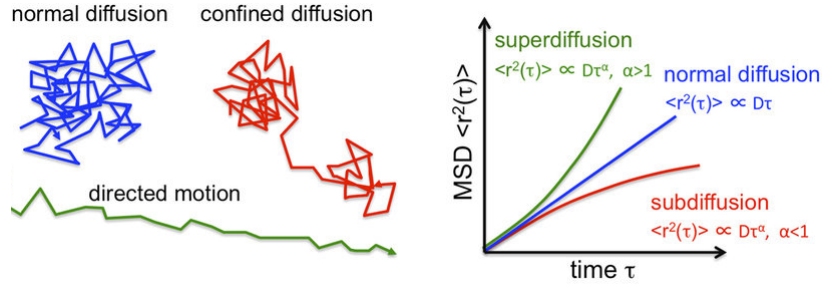
Figure 3.4: *Visual example of different behavior, adapted from [82].*

Neighbors analysis

Another interesting aspect in the formation of a confluent monolayer is the coordination number, id est the number of neighbors that each cell has at a given time. For a single layer, in hexatic symmetry is six, while for a two-layer is nine, due to three neighbors in the overlaying level, as described in Methods. Moreover, here the coordination is related to the final height of the system, as depicted in figure 3.5 where activity ζ and cell-cell adhesion ω_{cc} are used to map a parameter space representing the values of relative final z-coordinate.

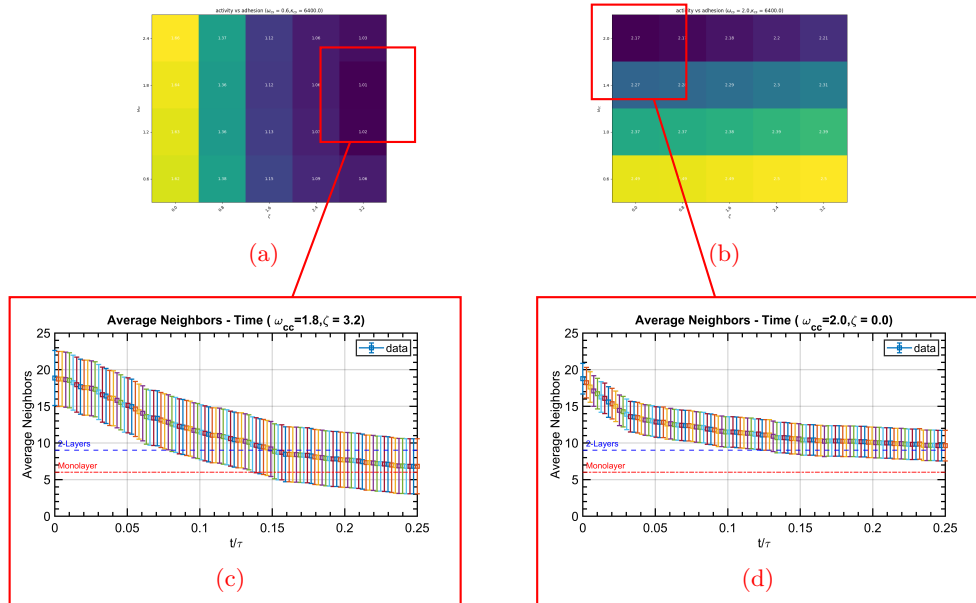**Figure 3.5:** *Parameter space of activity (ζ) against cell-cell adhesion (ω_{cc}) with respective final height of the system for two values of cell-substrate adhesion ($\omega_{cs} \in [0.6, 2.0]$) shown in (a) and (b), respectively*

Figure 3.5 is telling that the formation of a mono-layer is:

☞ ($\omega_{cs} = min(\omega_{cc})$) Tightly bound to the activity ζ rather than to the adhesion ω_{cc}. The system will develop towards a mono-layer when the activity is increasing as we can see in Figure 3.5(a).

☞ ($\omega_{cs} = max(\omega_{cc})$) The monolayer formation is not happening, as shown in 3.5(b). The system instead settles slowly in a two-layer configuration for lower ζ and higher ω_{cs}, while growing for any positive value of activity.

Where the monolayer state is associated with a value of coordination equal to 6 neighbors per cell on average while the missed formation is corresponding to 9. These values can be related to the height evolution of the system, namely a single layer is formed when the re-scaled height is closer to 1.0 [2] while two stable layers are present when its value is 2.0. Hereby, it should be noted that this system is tightly packed during initialization, therefore bringing the average initial height to 1.5, as can be seen in figure 3.6 where the two cases are shown. In fact, without activity, the system relaxes into two layers after growing, as shown in figure 3.6(b), while if active is going to achieve a single layer. Therefore, increasing the value of the activity, in a numerically stable range, provides transitions between two-to-one layer; the higher the activity is, the faster this transition occurs, whenever a certain threshold is crossed. In fact, the two states are both stable and form attractors for the system where its activity is used to discriminate between them, as can be seen in the appendix figure A.1.

(a)   (b)
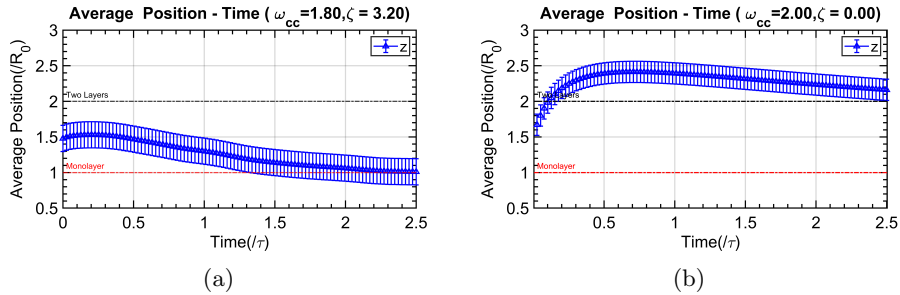
Figure 3.6: *Example of the evolution of the height of the system in two different scenarios: (a) Formation of a monolayer with $\omega_{cc} = 1.8$, $\omega_{cs} = 0.6$, $\zeta = 3.2$, and (b) Activity in a two layers system, not forming a monolayer with $\omega_{cc} = 2.0$, $\omega_{cs} = 2.0$, $\zeta = 0.0$.*

---

[2]Meaning that the mean position of the system, assigned through the center of mass ($c.o.m.$), is located at height $\langle h \rangle = radius$

Isotropic stress

This section is focusing on the development of isotropic stresses and their evolution over time. A more accurate description of these components is demanded later in the chapter where the setup results in clear behavior, but here the idea is to highlight a pattern that emerges during the formation of a monolayer, where the z-component of the stress, σ_z, increases above zero, that represents extension along the axis allowing vertical expansion of the cells which happens outward with respect to the substrate, that is impenetrable; while the system undergoes compression along the other main components, σ_x and σ_y, represented by the increasing negative value, as can be seen in figure 3.7. Once again, the activity plays a crucial role in determining their absolute value, since it represents the strength of the deformation. In fact, when the activity is removed, the stress components evolve around zero and do not allow the formation of a single layer.
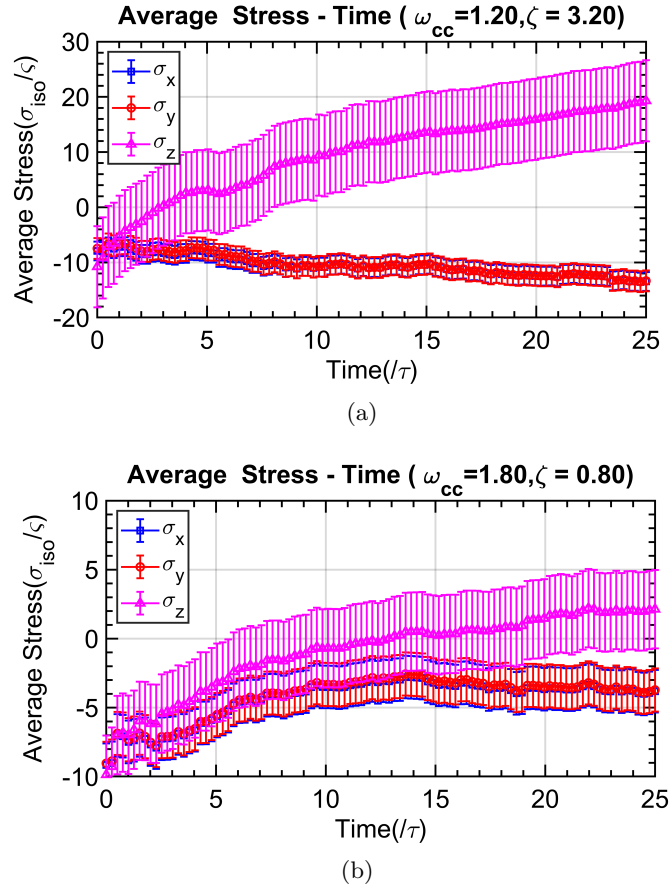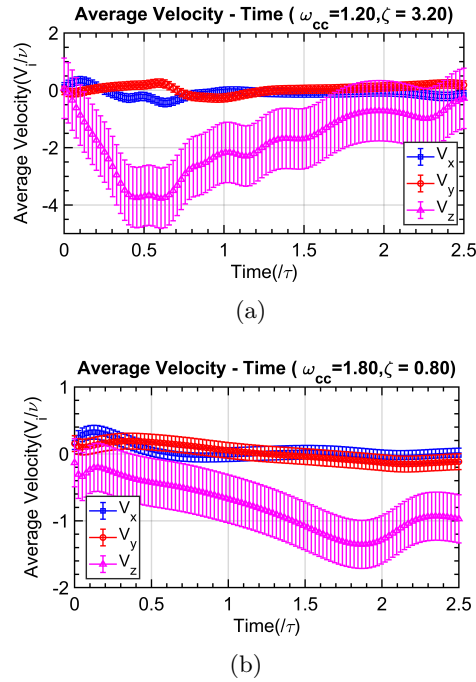

(a)

(b)

Figure 3.7: *Example of the evolution of the average stress of the system in two different scenarios: (a) Formation of a monolayer with $\omega_{cc} = 1.2$, $\omega_{cs} = 0.6$, $\zeta = 3.2$, and (b) Activity in a two layers system, not forming a monolayer with $\omega_{cc} = 1.8$, $\omega_{cs} = 0.6$, $\zeta = 0.8$.*

Velocity

As for the isotropic stress, more details will follow in the next section for clarity, and here are a few words to point out a pattern in the velocity profile that is common to the monolayer formation. The components parallel to the substrate, V_x and V_y oscillate around zero whenever the system is compact, meaning that the cells do not scatter away due to a combination of low adhesion and high activity, which is required for the formation of a confluent monolayer. Nonetheless, the greater oscillations happen at the beginning for high activity, that is the in-plane motion happens in the first part of the evolution, see figure 3.8, to settle in position right after and barely move once gaps are formed to allocate the upper cells.

The major deviation from zero happens across the vertical component V_z, where the negative sign stands for the direction of motion, id est towards the substrate. Once a minimum is reached, that happens fast, even the z-component tends towards zero, showing a deceleration in the process due to the interaction between the other cells and due to the active forces arising from cell deformation that are slowing down the formation. At the very end, every component stabilizes around zero, which means that the layer is *'frozen'* in place.

(a)

(b)

Figure 3.8: *Example of evolution of the average velocity components of the system in two different scenarios: (a) Formation of a monolayer with $\omega_{cc} = 1.2$, $\omega_{cs} = 0.6$, $\zeta = 3.2$, and (b) Activity in a two layers system, not forming a monolayer with $\omega_{cc} = 1.8$, $\omega_{cs} = 0.6$, $\zeta = 0.8$.*

Single cell interaction with a monolayer

To better understand how a cellular monolayer is formed, a single layer has been initialized with one cell on top of it, as depicted in figure 3.9(a). Changing values of cell-cell adhesion as well as activity is providing with a complete picture of how these factors influence morphogenesis. In other words, this system will provide an insight into the *mechanism* that drives cells from an upper layer to be incorporated into a single confluent layer by analyzing simple mechanical properties of the neighboring, underlying, cells.

(a)   (b)
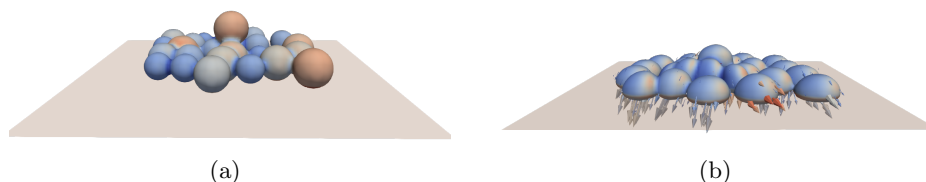
Figure 3.9: *Examples of the system in exam: (a): initialization of one layer of cells with one cell on top of it; (b): Formation of a single layer: the cells are merging while deforming; arrows represent the velocity field of the system. Colors represent stress magnitude: blue if low and red if high, while in light brown is depicted the substrate.*

Initialization

To set the stage, a proper initialization is carried over as a *passive process*, without any activity, in order for the system to settle. In fact, even if it is showing no motility, see figure 3.10, it is allowing a reorganization on a larger scale, from the velocity field to the stress field, the latter shown in figure 3.9.
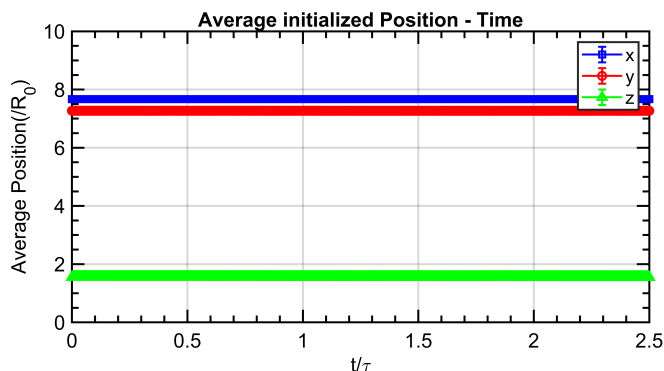
Figure 3.10: *Analysis of average positions during initialization*

Active system

Here, is shown how the activity is influencing the formation of a confluent layer.

First, by looking at how the average final height of the system is related to activity and to cell-cell adhesion, as shown in figure 3.11(a), by fixing cell-substrate adhesion at a low value, namely $\omega_{cs} = 0.06$:

☞ For $\zeta = max(\zeta)$ the system is showing strong numerical instabilities for any value of ω_{cc}, not allowing any analysis even right after the initialization;

☞ For $\zeta = min(\zeta)$ the evolution is smooth towards one layer, see figure 3.11(b), the uppermost cell is being incorporated into the lower layer while the other cells are deforming to better attach to the substrate[3]. The higher the value of cell-cell adhesion ω_{cc} the more compact the final system will be.

☞ For $min(\zeta) < \zeta < max(\zeta)$, the transition is dominated by cell motility, meaning that they are wandering around, see the left side of figure 3.11(b) where the height is oscillating back and forth, and even detach from one another before forming a single layer. This detachment, see figure 3.12, is inhibited for greater values of ω_{cc} while providing higher deformations[4], and explaining lower values of final height.

Seeing the behavior of the system as a whole, it is possible to analyze the mechanics of the neighbors of the upper cell[5]. Two major features are central for that purpose, namely the isotropic stress and the velocity. The overall behavior is represented in figures 3.13 and 3.17 where at time 5τ the uppermost cell is getting incorporated in the lower layer, see figures 3.11(b) and 3.11(b), making a switch in the z-component of the stress and velocity, meaning that both from decreasing they hit a 'minimum' and start increasing. This effect is due to the fact that in the very early time, the upper cell is just touching the lowers. therefore the system as a whole is trying to reach a stable configuration where the free energy is minimized. Some time has to pass in order for the perturbation to happen, namely the mechanical interactions between the cells due to the morphogenic event are taking place; from there the neighbors and the whole system are deforming and the behavior is changing until a *new* stability is reached where the cells have moved.
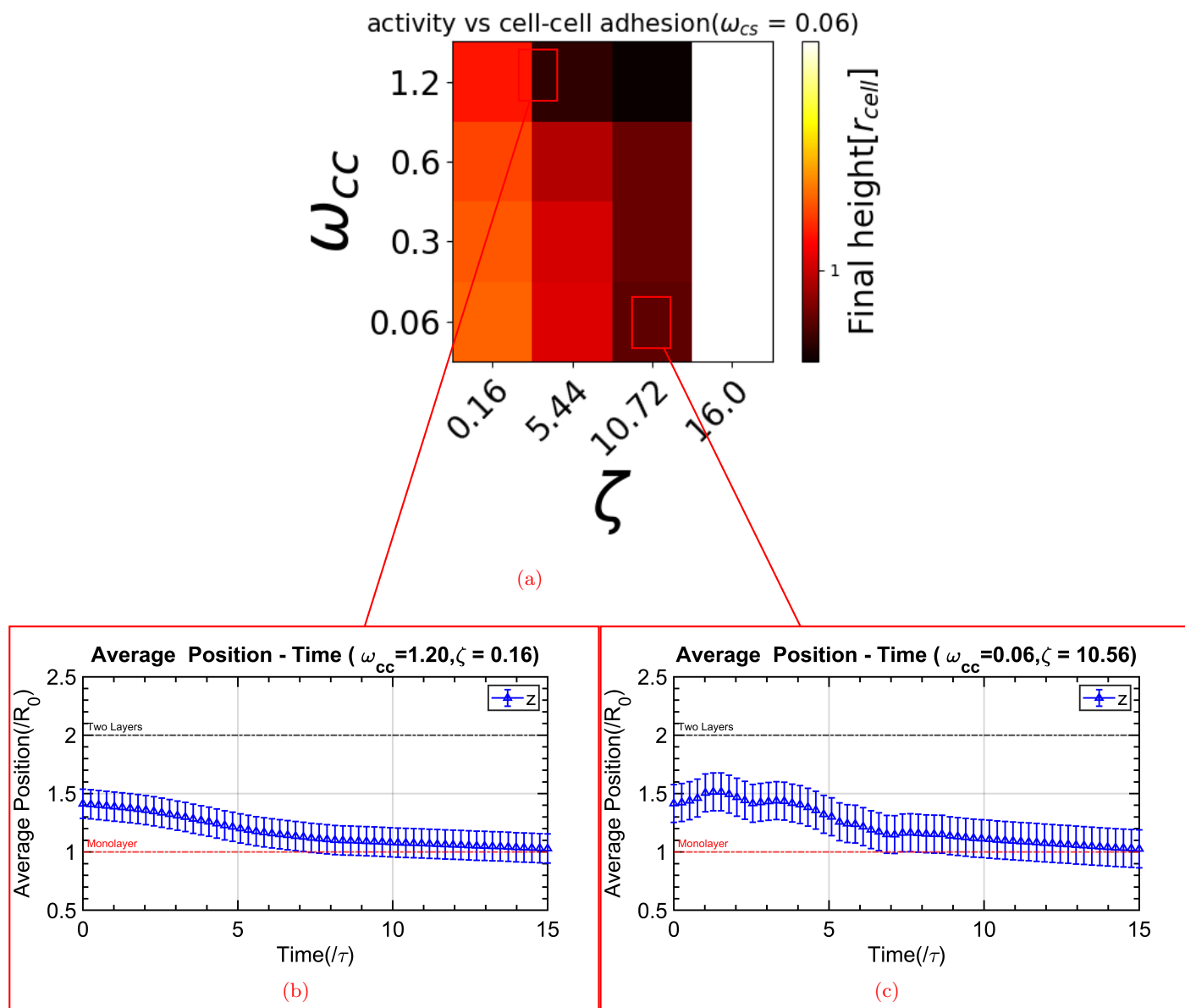
---

[3]The cell deformation is also the reason of the presence of values of final height lower than one.

[4]Tighter cells are pushing and pulling one another more providing greater stresses.

[5]Neighboring cells are hereby defined as cells within a cell diameter from the cell in the upper layer

Figure 3.11: *Parameter space of activity (ζ) against cell-cell adhesion (ω_{cc}) with respective final height of the system for cell-substrate adhesion $\omega_{cs} = 0.06$. In (b) $\omega_{cc} = 20\omega_{cs}$ and (c) $\omega_{cc} = \omega_{cs}$ is shown the height evolution of the system. For a higher level of activity, the system shows numerical instabilities and does not evolve from its initialized position, with a stripe in (a).*

<div align="center">(a) t=0   (b) t=5 τ (c) t=10 τ</div>
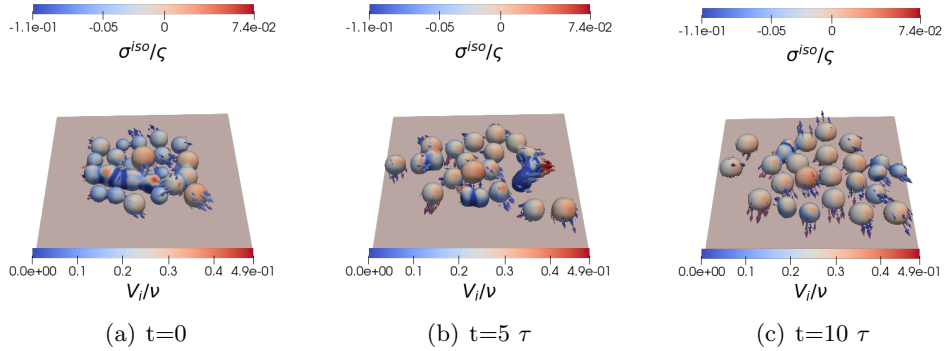
Figure 3.12: *Example of a high activity system, id est $\omega_{cc} = 0.6$, $\omega_{cs} = 0.06$, $\zeta = 5.4$, where the cells are wandering around before the formation of a single layer.*
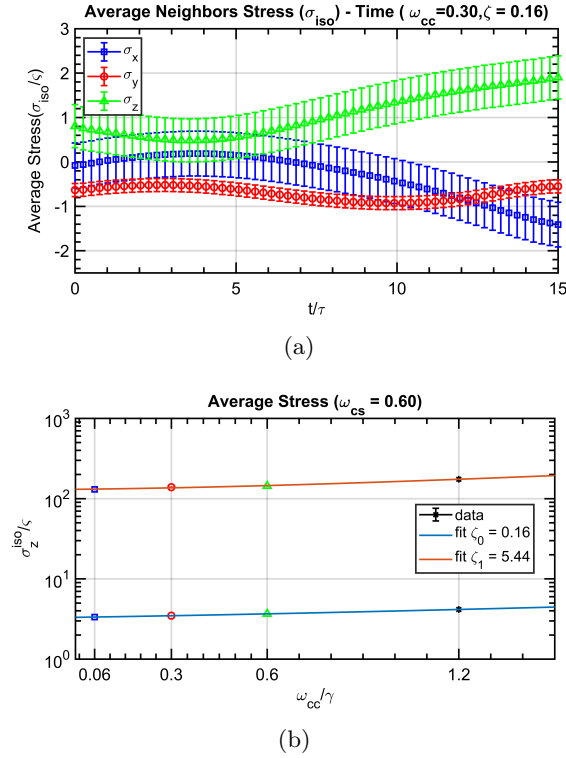
Stress

The stress profile, in figure 3.13(a), is remaining unchanged over different activity and cell-substrate adhesion values, while the magnitude of stresses is increasing accordingly to the activity, as can be seen in figure 3.13(b) where the final value is taken as a clear example; over time the value is behaving as shown on the side. The x- and y-components of the stress are negative, meaning that the cells are compressed in the respective direction, once a monolayer is formed; whereas the vertical component is increasing and positive which can be interpreted as the cells are expanding outside of the plane[6], once the merging has taken place. This is expressing that the incorporation of the cells into one layer is happening along the z-axis while relaxation is happening on the orthogonal directions of motion. Once the single layer is formed, if the activity is removed, the system will relax across all directions; in fact, returning stress values to their initial value around zero[7] when the activity alongside lower cell-substrate adhesion is scattering the cells away.

On the other side of the spectrum, a confluent layer is formed for lower values of activity and higher cells-substrate adhesion, as can be seen in the time evolution in figures 3.14, where the x- and y-stress components of neighboring cells do not reach a minimum in the same timescale but instead are going down, building up compression in the surroundings and expanding along the vertical axis, outside of the plain. This stress build-up is also the reason why the magnitude of the stresses is overall higher, nonetheless the overall profile is the same, as can be seen in figure 3.15.

[6]Remind that underneath the cells there is a solid undeformable substrate

[7]Note that the initial values of stress are in fact the values of the passive system after initialization.

(a)

(b)

Figure 3.13: *Examples of evolution of (a) isotropic stress for neighboring cells for fixed values of cell-cell adhesion and activity, while in (b) the average final stress for different values of cell-cell adhesion and activity for $\omega_{cs} = 0.06$*

Posing attention on the fact that the higher values of stress on the z-component, σ_z, are also due to the strong adhesion between cells, which is required for the compactness of the final state since the system is not in a dense state to begin with, while is surrounded by empty space to let the cells free to move. In fact, when cell activity is low, the uppermost cell has to push itself between other cells, deforming them; whereas at high ζ the cells are moving away from each other faster, leaving more empty space for the cells to merge in the single layer, as can be seen from the comparison between figure 3.14 and 3.12.

Remarkably, even lower levels of activity, for instance $\zeta = 0.03$ in figure 3.15(b), are not allowing the morphogenesis even for higher of adhesion, where instead the cells are deforming to adhere to the substrate while the uppermost cell is steadily over them. From this, the importance of activity is resulting clear as well as it is driving higher stresses on the neighboring cells which are nonetheless maintaining the same profile over different combinations of values.
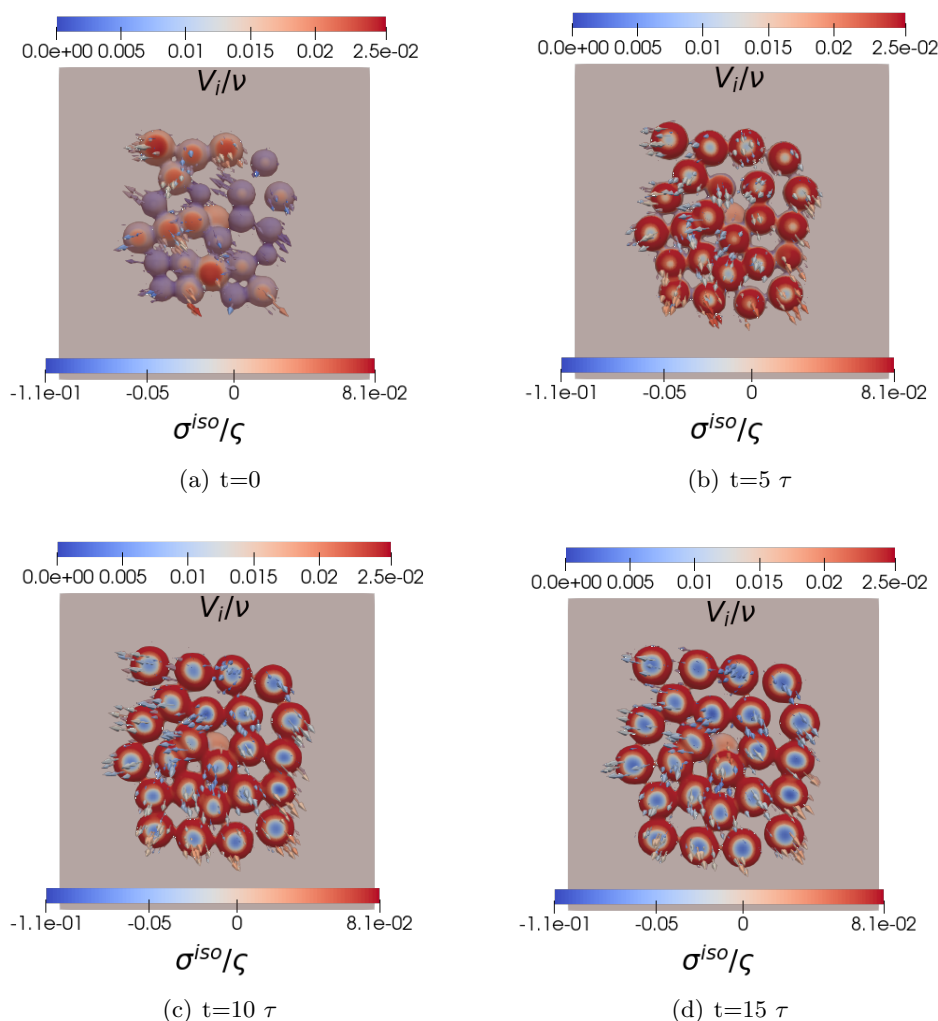
(a) t=5 τ (b) t=10 τ (c) t=15 τ
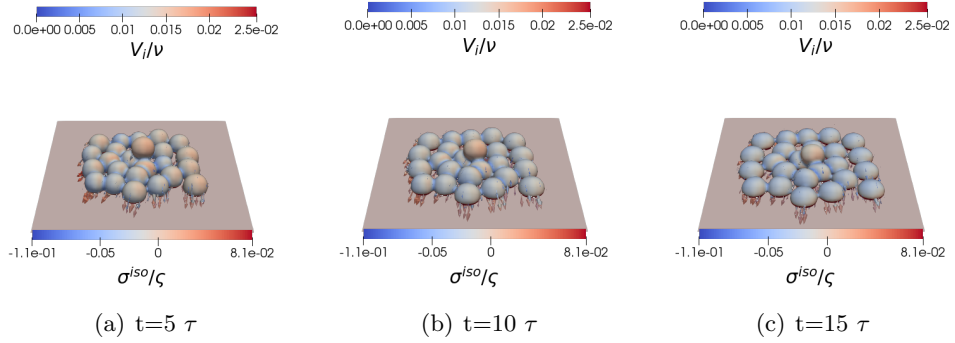
Figure 3.14: *Example of a low activity system, id est $\omega_{cc} = 0.4$, $\omega_{cs} = 0.08$, $\zeta = 0.16$, where the cells are confluent during the formation of a single layer.*

(a)   (b)
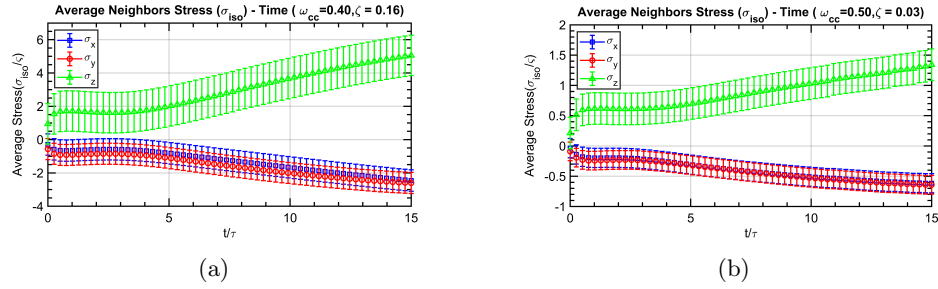
Figure 3.15: *Evolution of isotropic stress' components with (a) $\omega_{cs} = 0.08$ and (b) $\omega_{cs} = 0.1$, note the scale on the ordinate.*

Lastly, it has to be noted how the cells are behaving in contact with the solid substrate, an example can be seen in figure 3.16, where through the time evolution is possible to note another reason for the behavior of σ_z depicted above; in fact, since the cells cannot invaginate, it is contributing to the overall build-up of that component, Initially, the cells barely are touching the substrate, as depicted in figure 3.16(a); after a while, figure 3.16(b), they are coming in contact with it, building up positive stress that is mainly distributed on the edge due to the increasing forces exerted from the substrate onto the cells according to newton's third law, which is also causing deformation of the cells in accordance to the impenetrable scaffold setup and the outward deformation. In figure 3.16(c) and 3.16(d) has to be noted the negative stress components in the core of the cells that is pushing them inward providing an out-of-plane contribution to the maintenance of the droplet shape as stated by the volume constraint.

Remarkably, in the middle of the system can be seen greater deformations of the neighboring cells that have to adapt to incorporate the upper cell, further explaining the increase in their σ_z value. Moreover, this behavior is common to all confluent systems.

(a) t=0

(b) t=5 τ

(c) t=10 τ

(d) t=15 τ

Figure 3.16: *Example of a low activity system seen from below the substrate, id est $\omega_{cc} = 0.4$, $\omega_{cs} = 0.08$, $\zeta = 0.16$, where the cells are confluent during the formation of a single layer. Note that is the same system in 3.14. Positive stress stands for extensions and negative represents contractions with respect to the cell interface.*

Velocity

The velocity profile, shown in figure 3.17(a), is common to systems where a monolayer is formed and the neighboring cells are not scattering away too fast due to high activity, where instead the average end velocity is getting faster to zero due to a reduction of coordination between cells that are moving randomly as single cells do. In fact, once the cells are scattered away they tend to settle, as can be seen in the time evolution in figure 3.12 where first the cells move fast away from the others and then barely move.
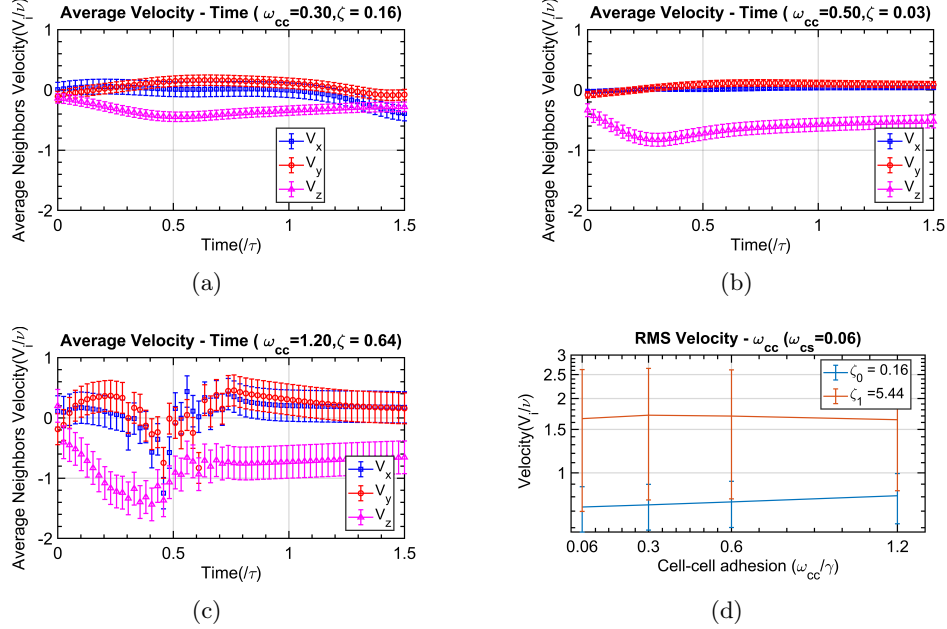
Figure 3.17: *Examples of evolution of velocity components for neighboring cells for (a) $\omega_{cs} = 0.06$, (b) $\omega_{cs} = 0.1$, and (c) $\omega_{cs} = 0.12$ while in (d) relation between RMS velocity and different values of cell-cell adhesion and activity*

On the other side of the spectrum, a monolayer is not formed due to low activity, even with higher adhesion values, as depicted in figure 3.18, is possible to note that the x- and y components of the velocity are oscillating near zero, as shown in figure 3.17(b), not allowing the cells to scatter away from their initial position while the in-plane component is negative, indicating that the interaction with the substrate tends to drive them closer to it.

From the very first time-step, the velocity field is pointing away from the cells, since it is not a stable configuration anymore when the activity is introduced into the system; but after a while, it is rearranging to drive them to the minimum of the free energy, that is different for different parameter but is well represented by the direction of the arrows in figures 3.18, 3.14, and 3.12 where the more active the more the on-plane, V_x, V_y, components are parallel to the substrate, can also be seen from the velocity average in figure 3.17. In the end, once a stable configuration is achieved, only the V_z component is nonzero but tending to it from below, reaching it whenever the activity and the interaction with the substrate are removed. If ζ and ω_{cc} are further increased, it is possible to notice a disruption in the continuity of the average velocity when the uppermost cell is getting incorporated, starting to interact with the neighbors, meaning that at higher values the morphogenesis might
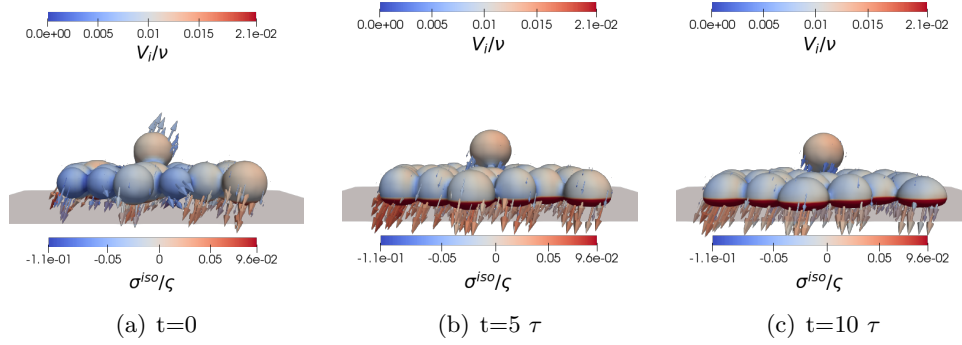
Figure 3.18: *Example of a low activity system, id est $\omega_{cc} = 0.5$, $\omega_{cs} = 0.1$, $\zeta = 0.03$, where the cells are not forming a monolayer.*

be happening roughly and the magnitude of the forces involved is spiking[8].

The level of activity of the system is crucial in determining its fate during the formation of a single layer: the higher the ζ is the greater the active driving forces are, implying larger velocity components. A fast cellular re-organization is promoting the formation of gaps in between the cells when the cell-substrate adhesion is low, allowing in-plane motion. A slow re-organization, also provided by a strong adhesion with the substrate is not allowing motion over the scaffold, *'locking'* the system in place. The monolayer formation is possible when gaps are present within the lower layer, places where other cells can be allocated. The intercellular adhesion is decisive in distinguishing between a single confluent layer and a single scattered layer.

---

[8]Remind that the cell velocity is related to the forces via the friction coefficient $v_i = \frac{\vec{F}_i^{tot}}{\xi}$

Chapter 4

Conclusion & Outlook

> It is wrong to think that the task of physics is to find out how nature is. Physics concerns what we can say about Nature.
>
> Niels Bohr

The current research aims to apply a quasi-three-dimensional phase field model developed for cells monolayer in the context of active matter to a greater plethora of physiological phenomena that take place in a full three-dimensional environment such as tissue morphogenesis, here used as a case study. Moreover, the understanding of the mechanics behind multi-layer cellular systems that are requiring both in-plane and out-of-plane forces has unveiled patterns in either velocity and stress profiles.

The ability of cells to convert chemical energy into mechanical forces, that allows them to move and modify their environment known as activity, has been put to the test in different scenarios, resulting effective and crucial even when the interactions are not just in-plane. In fact, this work has shown that cell activity is **required** in order to give a simple explanation of biological phenomena, and on that depends the fate of the system. This accounts for the increased interest in this branch of interdisciplinary physics in the last few decades.

Two simple interactions have been shown to capture the complexity of biology and a useful division between cells and substrate has shown the importance of the latter in tissue development: having a place to adhere provides a constraint to the direct motion while ensuring the ability to reorganize in a more energy-convenient configuration.

A cellular system evolves towards the minimum of free energy in order to reach the stability that can be seen in nature at the same time perturbations drive it out of equilibrium in this case through ζ, and by modifying

the surroundings a new stability will be reached, and so forth giving birth to cycles.

This points out the importance of being out of equilibrium, where things might be difficult to understand, but thanks to simple models it is possible to grasp the behavior of Nature. In this case thanks to active matter it has been shown how it is possible to dive into the morphogenesis.

To briefly sum up, a mathematical, phase-field model of active droplets was applied to a two-layer cellular system to demonstrate that it can be used to describe tissue development in a three-dimensional environment. That was a missing fragment in previous writings. This provides a new tool to approach cellular dynamics in the context of collective behavior in a biophysical sense. The analysis of the results has shown the importance of cellular activity in shaping the fate of the cellular system in a physiological phenomenon.

The role of mechanical forces is crucial to understanding tissue morphogenesis. This research has shown how simple mechanical features such as *isotropic stress* and *velocity profile* are shaped by the ability of the cells of performing work on the surrounding, giving rise to precise patterns, independent of the size of the system but rather depending on how active the system is. Not less important are the interactions with the substrate that has been shown to promote different states, namely:

☞ too low adhesion ω_{cs} alongside some activity ζ are driving towards a scattered final state, where cells are away from one another;

☞ too high adhesion is locking the system in place, not allowing cells to move, even when the activity is resulting higher;

☞ For intermediate values of adhesion, the activity is decisive to set the timescale of morphogenesis;

☞ At very high activity the system has shown non-physical behaviors even for higher values of cell-substrate adhesion.

The study is in its early stage and limited by the choice of the parameters that are embedded in the biological apparatus behind the physiological process, such as the strength of adhesion, which is different for different junctions, and which is here considered constant for all the cells for each simulation. To a greater extent differential activity across layers where some of them are passive while others are changing over time. Another important aspect is the approximation of cells being all the same. In fact, the shape is as different as the interface between them, as well as their rigidity that changes, while here it is fixed. Another limiting aspect is the finite size effect: the cellular system considered here was pretty small compared to the thousands of cells that form a real cell cluster.

A major limiting factor is to relate these results with real experiments: what can be compared is the overall behavior for different scenarios since

spurious values have to be taken *cum grano salis* even if the effort to make them comparable has been made, making dimensionless quantities. Lastly, this model is deterministic, while in Nature noise might help to drive the system out of equilibrium and even factors outside of the cell may initiate a chain reaction. On the other hand, there is the importance of the substrate stiffness and shape that has not been explored here, as well as the different substances or constraints that are surrounding the system.

Nonetheless, this is a first step in what seems to be the right direction for describing living tissues with active matter, making a jump to a fully three-dimensional system, even if with a simple model of collective behavior.

Therefore, this can open the door to future developments which can start by removing some limits to the study, such as the implementation of different levels of activity and cell-cell adhesion across different layers to extend the applicability of the model to more complex systems, which can also be described with the introduction of other active driving forces such as polarization. Future studies could fruitfully explore this issue further by changing the shape of the scaffold as well as allowing cells to invaginate into it by changing its rigidity. Future research on the parameter space $\omega_{cs} vs \zeta$, for longer times, might reveal a sharper threshold for the formation of a single layer as well as provide a possible relation between activity and the timescale of the self-organization. In future work, investigating the pattern formed by the stresses and velocities might prove important, either experimentally and theoretically in an effort to understand the interdependence between their magnitude and the physiological changes that are happening inside and outside of the cell. Developments of the model may look into different geometries and configurations for both cells and substrate, extending its validity. Future studies can also couple the mechanics with fluid flows outside of the system as well as introduce different components to simulate the effect of biochemical signaling and different drugs.

I look forward to reading further attempts which could prove quite beneficial to the subject under discussion.

Appendix A

Appendix

New cell-cell adhesion and example of calculation

$$\mathcal{F}_{adh} = \sum_i^N \sum_{j\neq i} \omega\lambda \int d\vec{x}(\nabla\phi_i)^2 \cdot (\nabla\phi_j)^2 \tag{A.1}$$

$$\frac{\delta\mathcal{F}_{adh}}{\delta\phi_i} = \frac{\partial\mathcal{F}_{adh}}{\partial\phi_i} - \nabla \cdot \frac{\partial\mathcal{F}_{adh}}{\partial\nabla\phi_i} \tag{A.2}$$

$$\text{observing}: \quad \frac{\partial\mathcal{F}_{adh}}{\partial\phi_i} = 0 \tag{A.3}$$

$$\text{while}: \quad \frac{\partial\mathcal{F}_{adh}}{\partial\nabla\phi_i} = \sum_{j\neq i} \omega\lambda 2 * \nabla\phi_i \cdot (\nabla\phi_j)^2 \tag{A.4}$$

Since $\nabla \cdot (\vec{a} \cdot \vec{b}) = \nabla(\vec{a} \cdot \vec{b}) = \vec{a} \cdot \nabla\vec{b} + \vec{b} \cdot \nabla\vec{a}$
Follows:

$$\frac{\delta\mathcal{F}_{adh}}{\delta\phi_i} = -\nabla \cdot (\sum_{j\neq i} \omega\lambda 2 * \nabla\phi_i \cdot (\nabla\phi_j)^2) \tag{A.5}$$

$$= -\sum_{j\neq i} 2\omega\lambda[\nabla \cdot (\nabla\phi_i \cdot (\nabla\phi_j)^2)] \tag{A.6}$$

$$= -\sum_{j\neq i} 2\omega\lambda[\nabla(\nabla\phi_i \cdot (\nabla\phi_j)^2)] \tag{A.7}$$

$$= -\sum_{j\neq i} 2\omega\lambda[\nabla^2\phi_i \cdot (\nabla\phi_j)^2 + \nabla\phi_i \cdot 2(\nabla\phi_j\nabla^2\phi_j))] \tag{A.8}$$

$$= -\sum_{j\neq i} 2\omega\lambda\nabla\phi_j[\nabla^2\phi_i \cdot \nabla\phi_j + \nabla\phi_i \cdot 2\nabla^2\phi_j] \tag{A.9}$$

$$= -2\omega\lambda\nabla\phi_i[\nabla\phi_i(\sum_i^N \nabla^2\phi_i - \nabla^2\phi_i) + 2\nabla^2\phi_i(\sum_i^N \nabla\phi_i - \nabla\phi_i)] \tag{A.10}$$

Where in the last equality is used $\sum_{j\neq i} \mathcal{G}_j = \sum_i^N \mathcal{G}_i - \mathcal{G}_i$ with $\mathcal{G} = \nabla^2\phi$ and $\nabla\phi$ respectively

Height evolution versus activity
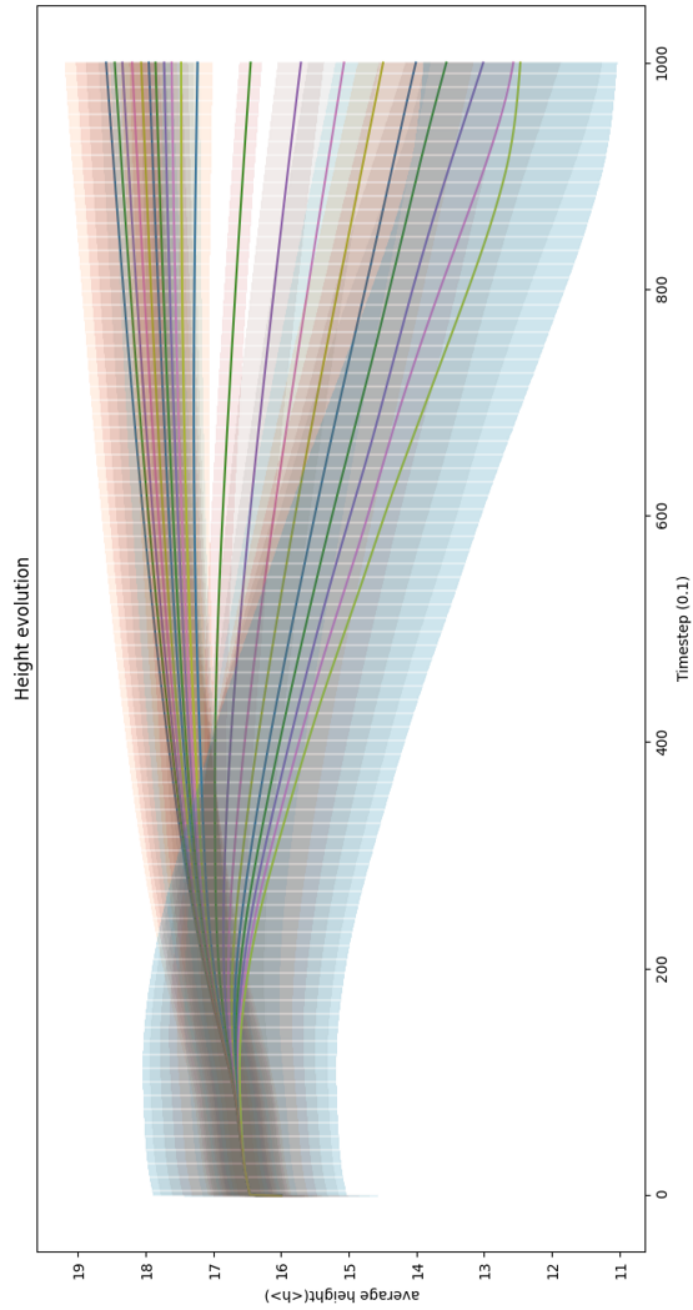
Figure A.1: *Activity is deciding the fate of the system, from top to bottom it is changing from $\zeta = 0.0$ at the top to $\zeta = high$ at the bottom.*

Bibliography

[1] V. Hakim and P. Silberzan. "*Collective cell migration: a physics perspective*". In: *Rep. Prog. Phys.* **80**.076601 (2017). DOI: https://doi.org/10.1088/1361-6633/aa65ef.

[2] O. Du Roure et al. "*Force mapping in epithelial cell migration*". In: *Proc. Natl. Acad. Sci. U.S.A.* **102**.7 (2005), pp. 2390–2395. DOI: https://doi.org/10.1073/pnas.0408482102.

[3] Poul M Bendix et al. "A quantitative analysis of contractility in active cytoskeletal protein networks". In: *Biophysical journal* 94.8 (2008), pp. 3126–3136.

[4] Xavier Trepat et al. "Physical forces during collective cell migration". In: *Nature physics* 5.6 (2009), pp. 426–430.

[5] M Cristina Marchetti et al. "Hydrodynamics of soft active matter". In: *Reviews of modern physics* 85.3 (2013), p. 1143.

[6] Carles Blanch-Mercader et al. "Turbulent dynamics of epithelial cell cultures". In: *Physical review letters* 120.20 (2018), p. 208101.

[7] Kevin Chiou and Eva-Maria S. Collins. "Why we need mechanics to understand animal regeneration". In: *Developmental Biology* 433.2 (2018). Regeneration: from cells to tissues to organisms, pp. 155–165. ISSN: 0012-1606. DOI: https://doi.org/10.1016/j.ydbio.2017.09.021. URL: https://www.sciencedirect.com/science/article/pii/S0012160617303500.

[8] Agustí Brugués et al. "Forces driving epithelial wound healing". In: *Nature physics* 10.9 (2014), pp. 683–690.

[9] Chiara De Pascalis and Sandrine Etienne-Manneville. "Single and collective cell migration: the mechanics of adhesions". In: *Molecular biology of the cell* 28.14 (2017), pp. 1833–1846.

[10] Peter Friedl et al. "Classifying collective cancer cell invasion". In: *Nature cell biology* 14.8 (2012), pp. 777–783.

[11] Anders E Carlsson. "Actin dynamics: from nanoscale to microscale". In: *Annual review of biophysics* 39 (2010), pp. 91–110.

[12]　Stacey A Maskarinec et al. "Quantifying cellular traction forces in three dimensions". In: *Proceedings of the National Academy of Sciences* 106.52 (2009), pp. 22108–22113.

[13]　Benoit Ladoux. "Cells guided on their journey". In: *Nature Physics* 5.6 (2009), pp. 377–378.

[14]　Benoit Ladoux and René-Marc Mège. "Mechanobiology of collective cell behaviours". In: *Nature reviews Molecular cell biology* 18.12 (2017), pp. 743–757.

[15]　Minerva Bosch-Fortea and Fernando Martín-Belmonte. "Mechanosensitive adhesion complexes in epithelial architecture and cancer onset". In: *Current Opinion in Cell Biology* 50 (2018), pp. 42–49.

[16]　Y. A. Miroshnikova et al. "*Adhesion forces and cortical tension couple cell proliferation and differentiation to drive epidermal stratification*". In: *Nat. Cell. Biol.* **20** (2018), pp. 69–80. DOI: https://doi.org/10.1038/s41556-017-0005-z.

[17]　Camelia G Tusan et al. "Collective cell behavior in mechanosensing of substrate thickness". In: *Biophysical journal* 114.11 (2018), pp. 2743–2755.

[18]　Jieling Zhao, Farid Manuchehrfar, and Jie Liang. "Cell–substrate mechanics guide collective cell migration through intercellular adhesion: a dynamic finite element cellular model". In: *Biomechanics and modeling in mechanobiology* 19.5 (2020), pp. 1781–1796.

[19]　Kelly Vazquez, Aashrith Saraswathibhatla, and Jacob Notbohm. "Effect of substrate stiffness on friction in collective cell migration". In: *Scientific Reports* 12.1 (2022), p. 2474.

[20]　Lakshmi Balasubramaniam et al. "Investigating the nature of active forces in tissues reveals how contractile cells can form extensile monolayers". In: *Nature materials* 20.8 (2021), pp. 1156–1166.

[21]　Julia M. Yeomans Romain Mueller and Amin Doostmohammadi. "*Emergence of Active Nematic Behavior in Monolayers of Isotropic Cells*". In: *Phys. Rev. Lett.* **122**.048004 (2019). DOI: 10.1103/PhysRevLett.122.048004.

[22]　Ulrike Schnell, Vincenzo Cirulli, and Ben NG Giepmans. "EpCAM: structure and function in health and disease". In: *Biochimica et Biophysica Acta (BBA)-Biomembranes* 1828.8 (2013), pp. 1989–2001.

[23]　Barry M Gumbiner. "Cell adhesion: the molecular basis of tissue architecture and morphogenesis". In: *Cell* 84.3 (1996), pp. 345–357.

[24]　Stephen Bustin. *Molecular biology of the cell, ; ISBN: 9780815344643; and molecular biology of the cell, the problems book; ISBN 9780815344537.* 2015.

[25] Anna Huttenlocher, Rebecca R Sandborg, and Alan F Horwitz. "Adhesion in cell migration". In: *Current opinion in cell biology* 7.5 (1995), pp. 697–706.

[26] Fiona N Kenny and John T Connelly. "Integrin-mediated adhesion and mechano-sensing in cutaneous wound healing". In: *Cell and tissue research* 360 (2015), pp. 571–582.

[27] Tomaz Velnar, Tracey Bailey, and Vladimir Smrkolj. "The wound healing process: an overview of the cellular and molecular mechanisms". In: *Journal of international medical research* 37.5 (2009), pp. 1528–1542.

[28] Yan Zhang, Gail Reif, and Darren P Wallace. "Extracellular matrix, integrins, and focal adhesion signaling in polycystic kidney disease". In: *Cellular signalling* 72 (2020), p. 109646.

[29] Valeriia Grudtsyna et al. "Extracellular matrix sensing via modulation of orientational order of integrins and F-actin in focal adhesions". In: *Life Science Alliance* 6.10 (2023).

[30] Annette Trommler, David Gingell, and H Wolf. "Red blood cells experience electrostatic repulsion but make molecular adhesions with glass". In: *Biophysical journal* 48.5 (1985), pp. 835–841.

[31] David M Bryant and Keith E Mostov. "From cells to organs: building polarized tissue". In: *Nature reviews Molecular cell biology* 9.11 (2008), pp. 887–901.

[32] Mary C Halloran and Marc A Wolman. "Repulsion or adhesion: receptors make the call". In: *Current opinion in cell biology* 18.5 (2006), pp. 533–540.

[33] Rüdiger Klein. "Eph/ephrin signaling in morphogenesis, neural development and plasticity". In: *Current opinion in cell biology* 16.5 (2004), pp. 580–589.

[34] Scott E Williams et al. "Ephrin-B2 and EphB1 mediate retinal axon divergence at the optic chiasm". In: *Neuron* 39.6 (2003), pp. 919–935.

[35] W. Ning et al. "*Differentiated Daughter Cells Regulate Stem Cell Proliferation and Fate through Intra-tissue Tension*". In: *Cell Stem Cell* **28** (2021), pp. 1–17. DOI: https://doi.org/10.1016/j.stem.2020.11.002.

[36] Florian Milde et al. "SEM++: A particle model of cellular growth, signaling and migration". In: *Computational Particle Mechanics* 1 (2014), pp. 211–227.

[37] John Metzcar et al. "A review of cell-based computational modeling in cancer biology". In: *JCO clinical cancer informatics* 2 (2019), pp. 1–13.

[38] Jonas Pleyer and Christian Fleck. "Agent-based models in cellular systems". In: *Frontiers in Physics* 10 (2023), p. 1337.

[39] Aleksandra Ardaševa et al. "Comparative study between discrete and continuum models for the evolution of competing phenotype-structured cell populations in dynamical environments". In: *Physical Review E* 102.4 (2020), p. 042404.

[40] Gerard A Ateshian et al. "Continuum modeling of biological tissue growth by cell division, and alteration of intracellular osmolytes and extracellular fixed charge density". In: (2009).

[41] Shuji Ishihara, Philippe Marcq, and Kaoru Sugimura. "From cells to tissue: A continuum model of epithelial mechanics". In: *Physical Review E* 96.2 (2017), p. 022418.

[42] Naoki Kida and Yoshihiro Morishita. "Continuum mechanical modeling of developing epithelial tissues with anisotropic surface growth". In: *Finite Elements in Analysis and Design* 144 (2018), pp. 49–60.

[43] Soheil Firooz et al. "On continuum modeling of cell aggregation phenomena". In: *Journal of the Mechanics and Physics of Solids* 167 (2022), p. 105004.

[44] Maud El-Hachem, Scott W McCue, and Matthew J Simpson. "A continuum mathematical model of substrate-mediated tissue growth". In: *Bulletin of Mathematical Biology* 84.4 (2022), p. 49.

[45] Zhiqiang Bi and Robert F Sekerka. "Phase-field model of solidification of a binary alloy". In: *Physica A: Statistical Mechanics and its Applications* 261.1-2 (1998), pp. 95–106.

[46] JS Langer. "Models of pattern formation in first-order phase transitions". In: *Directions in condensed matter physics: Memorial volume in honor of shang-keng ma*. World Scientific, 1986, pp. 165–186.

[47] Falko Ziebert, Sumanth Swaminathan, and Igor S Aranson. "Model for self-polarization and motility of keratocyte fragments". In: *Journal of The Royal Society Interface* 9.70 (2012), pp. 1084–1092.

[48] Sara Najem and Martin Grant. "Phase-field model for collective cell migration". In: *Physical Review E* 93.5 (2016), p. 052405.

[49] Benoit Palmieri et al. "Multiple scale model for cell migration in monolayers: Elastic mismatch between cells enhances motility". In: *Scientific reports* 5.1 (2015), p. 11745.

[50] Makiko Nonomura. "Study on multicellular systems using a phase field model". In: *PloS one* 7.4 (2012), e33501.

[51] Robert Chojowski, Ulrich S Schwarz, and Falko Ziebert. "Reversible elastic phase field approach and application to cell monolayers". In: *The European Physical Journal E* 43 (2020), pp. 1–12.

[52] Romain Mueller and Amin Doostmohammadi. "*Phase field models of active matter*". In: *arXiv.org* (2021). DOI: 10.48550/arxiv.2102.05557.

[53] Siavash Monfared and Amin Doostmohammadi et al. "*Mechanical basis and topological routes to cell elimination*". In: *Elife* **12** (2023), e82435.

[54] Ricard Alert and Xavier Trepat. "Physical models of collective cell migration". In: *Annual Review of Condensed Matter Physics* 11 (2020), pp. 77–101.

[55] Adrian Moure and Hector Gomez. "Phase-field modeling of individual and collective cell migration". In: *Archives of Computational Methods in Engineering* 28 (2021), pp. 311–344.

[56] Apratim Bajpai et al. "The interplay between cell-cell and cell-matrix forces regulates cell migration dynamics". In: *Biophysical journal* 117.10 (2019), pp. 1795–1804.

[57] K. R. Mesa et al. "*Homeostatic Epidermal Stem Cell Self-Renewal Is Driven by Local Differentiation*". In: *Cell Stem Cell* **23** (2018), pp. 677–686. DOI: https://doi.org/10.1016/j.stem.2018.09.005.

[58] M. Rubsam et al. "*E-cadherin integrates mechanotransduction and EGFR signaling to control junctional tissue polarization and tight junction positioning*". In: *Nat. Comm.* **8**.1250 (2017). DOI: 10.1038/s41467-017-01170-7.

[59] Toshiyuki Koyama. "Phase Field". In: *Springer Handbook of Materials Measurement Methods*. Ed. by Horst Czichos, Tetsuya Saito, and Leslie Smith. Berlin, Heidelberg: Springer Berlin Heidelberg, 2006, pp. 1031–1055. ISBN: 978-3-540-30300-8. DOI: 10.1007/978-3-540-30300-8_21. URL: https://doi.org/10.1007/978-3-540-30300-8_21.

[60] Adam A Wheeler, William J Boettinger, and Geoffrey B McFadden. "Phase-field model for isothermal phase transitions in binary alloys". In: *Physical Review A* 45.10 (1992), p. 7424.

[61] Thuan Beng Saw et al. "Topological defects in epithelia govern cell death and extrusion". In: *Nature* 544.7649 (2017), pp. 212–216.

[62] Michael E Cates and Elsen Tjhung. "Theories of binary fluid mixtures: from phase-separation kinetics to active emulsions". In: *Journal of Fluid Mechanics* 836 (2018), P1.

[63] Frank Jülicher, Stephan W Grill, and Guillaume Salbreux. "Hydrodynamic theory of active matter". In: *Reports on Progress in Physics* 81.7 (2018), p. 076601.

[64] Amin Doostmohammadi et al. "Active nematics". In: *Nature communications* 9.1 (2018), p. 3246.

[65] Kyogo Kawaguchi, Ryoichiro Kageyama, and Masaki Sano. "Topological defects control collective dynamics in neural progenitor cell cultures". In: *Nature* 545.7654 (2017), pp. 327–331.

[66] G Duclos et al. "Spontaneous shear flow in confined cellular nematics". In: *Nature physics* 14.7 (2018), pp. 728–732.

[67] Ludwig A Hoffmann et al. "Theory of defect-mediated morphogenesis". In: *Science Advances* 8.15 (2022), eabk2712.

[68] Ananyo Maitra, Martin Lenz, and Raphael Voituriez. "Chiral active hexatics: Giant number fluctuations, waves, and destruction of order". In: *Physical Review Letters* 125.23 (2020), p. 238005.

[69] Anshuman Pasupalak et al. "Hexatic phase in a model of active biological tissues". In: *Soft matter* 16.16 (2020), pp. 3914–3920.

[70] John W. Cahn and John E. Hilliard. "*Free Energy of a Nonuniform System. I. Interfacial Free Energy*". In: *J. Chem. Phys.* **28** (1958), pp. 258–267. DOI: https://doi.org/10.1063/1.1744102.

[71] Samuel Miller Allen and John W Cahn. "Ground state structures in ordered binary alloys with second neighbor interactions". In: *Acta Metallurgica* 20.3 (1972), pp. 423–433.

[72] Brian A Camley and Wouter-Jan Rappel. "Physical models of collective cell motility: from cell to tissue". In: *Journal of physics D: Applied physics* 50.11 (2017), p. 113002.

[73] Igor S Aranson. *Physical models of cell motility.* Springer, 2016.

[74] Siavash Monfared et al. "Stress percolation criticality of glass to fluid transition in active cell layers". In: *arXiv preprint arXiv:2210.08112* (2022).

[75] Aleksandra Ardaševa, Romain Mueller, and Amin Doostmohammadi. "Bridging microscopic cell dynamics to nematohydrodynamics of cell monolayers". In: *arXiv preprint arXiv:2204.12994* (2022).

[76] Chenlu Wang et al. "The interplay of cell-cell and cell-substrate adhesion in collective cell migration". In: *Journal of The Royal Society Interface* 11.100 (2014), p. 20140684.

[77] Bingcheng Yi, Qi Xu, and Wei Liu. "An overview of substrate stiffness guided cellular response and its applications in tissue regeneration". In: *Bioactive materials* 15 (2022), pp. 82–102.

[78] Jae Hun Kim et al. "Propulsion and navigation within the advancing monolayer sheet". In: *Nature materials* 12.9 (2013), pp. 856–863.

[79] Shiladitya Banerjee and M Cristina Marchetti. "Continuum models of collective cell migration". In: *Cell Migrations: Causes and Functions* (2019), pp. 45–66.

[80] Guanming Zhang and Julia M Yeomans. "Active forces in confluent cell monolayers". In: *Physical Review Letters* 130.3 (2023), p. 038202.

[81] Marius Asipauskas et al. "A texture tensor to quantify deformations: the example of two-dimensional flowing foams". In: *Granular Matter* 5.2 (2003), pp. 71–74.

[82] Achillefs N Kapanidis, Stephan Uphoff, and Mathew Stracy. "Understanding protein mobility in bacteria by tracking single molecules". In: *Journal of Molecular Biology* 430.22 (2018), pp. 4443–4455.